

**ANALYTICAL IMPROVEMENTS IN THE DETECTION OF AMYLOID- $\beta$  PEPTIDES IN  
CEREBROSPINAL FLUID BY MASS SPECTROMETRY**

by

Quyen Nguyen

B.Sc., The University of British Columbia, 2016

A THESIS SUBMITTED IN PARTIAL FULFILLMENT OF  
THE REQUIREMENTS FOR THE DEGREE OF

MASTER OF SCIENCE

in

THE FACULTY OF GRADUATE AND POSTDOCTORAL STUDIES  
(Pathology and Laboratory Medicine)

THE UNIVERSITY OF BRITISH COLUMBIA  
(Vancouver)

August 2019

© Quyen Nguyen, 2019

The following individuals certify that they have read, and recommend to the Faculty of Graduate and Postdoctoral Studies for acceptance, a thesis/dissertation entitled:

Analytical improvements in the detection of amyloid- $\beta$  peptides in cerebrospinal fluid by mass spectrometry

---

submitted by Quyen (Amy) Nguyen in partial fulfillment of the requirements for

the degree of Master of Science

in Pathology and Laboratory Medicine

**Examining Committee:**

Mari DeMarco, Pathology and Laboratory Medicine  
Supervisor

Philipp Lange, Pathology and Laboratory Medicine  
Supervisory Committee Member

Haakon Nygaard, Clinic for Alzheimer and Related Disorder  
Supervisory Committee Member

Vilte Barakauskas, Pathology and Laboratory Medicine  
Additional Examiner

**Additional Supervisory Committee Members:**

Honglin Luo, Pathology and Laboratory Medicine  
Supervisory Committee Member

Supervisory Committee Member

## Abstract

Current diagnosis of Alzheimer's disease (AD) is based on physical and neurological exams, mental state exams, and brain scans. Cerebrospinal fluid (CSF) biomarkers such as amyloid- $\beta$  ( $A\beta$ ) peptides have been incorporated into the research diagnostic criteria for AD and clinical care.  $A\beta$  peptides are produced from the amyloid precursor protein (APP) by proteolytic cleavage.  $A\beta$ 40 and  $A\beta$ 42, along with the protein tau, are reliable biochemical indicators of AD. Additionally autosomal dominant AD is caused from highly penetrant autosomal dominantly inherited variants in the *APP*, presenilin 1 and 2 genes.

Biomarker detection and quantification is commonly performed by immunoassays, which provide an indirect measurement of the analyte of interest. In the case of  $A\beta$  immunoassays, high between-lab variability and lack of harmonization between platforms has been a concern. Moreover, immunoassays are known, in general, to be prone to analytical interferences – both positive and negative – from endogenous and exogenous molecules.

To overcome issues associated with antibody-based detection methods and the desire to implement AD biomarker testing in routine care, a liquid chromatography tandem mass spectrometry (LC-MS/MS) assay was previously developed by the laboratory for detecting evidence of AD pathology by quantifying wild-type  $A\beta$ 40 and  $A\beta$ 42 in CSF.

The aims of this thesis with respect to the LC-MS/MS method were to (1) evaluate the surrogate matrix composition, investigate potential interferences, and identify criteria for sample acceptance/rejection in a clinical environment, and (2) to adapt the method from detecting wild-type A $\beta$  peptides to also detecting A $\beta$  variants. The surrogate matrix was established with protein content compatible with that observed in human CSF. The interference studies indicated all endogenous and exogenous factors tested met the pre-specified bias acceptance criteria for A $\beta$ 40 and A $\beta$ 42. Thus A $\beta$  peptides can be accurately quantified in the presence of high but physiologically plausible total protein concentrations and anti-A $\beta$  antibodies, enabling use in routine clinical care and clinical trials. Additionally, testing hemolysate contaminated samples indicated no interference from hemolysate in the range commonly seen by the clinical laboratory. The LC-MS/MS assay was adapted to quantify wild type-A $\beta$ 42, A $\beta$ 40 and to identify A $\beta$  variants in CSF.

## **Lay Summary**

Alzheimer's disease (AD) is characterized by the presence of protein clusters in the brain formed by a peptide called amyloid- $\beta$  ( $A\beta$ ). There is evidence that measuring the amount of  $A\beta$  peptides, more specifically  $A\beta_{42}$ , in the fluid surrounding the brain, cerebrospinal fluid (CSF), can be indicative of cognitive decline due to AD. To measure  $A\beta$ , a technique called mass spectrometry can be used to detect and measure the amount of specific peptides present based on their mass. The objectives of this thesis were to evaluate factors such as blood, protein, and therapeutics compounds that can potentially cause interference and to adapt a previous developed method to measure both  $A\beta$  peptides and familial variants in CSF using a highly selective technique. The knowledge gained from this research aims to improve diagnostic testing for AD and related disorders.

## **Preface**

The work presented herein was conducted as part of the research group of Dr. Mari DeMarco in the Department of Pathology and Laboratory Medicine at the University of British Columbia. In addition to the support of the research group, I would like to specifically acknowledge the contributions of Ms. Grace van der Gugten (Providence Health Care), Ms. Alice Fok, and Dr. Robin Hsiung to this work.

Chapter 2 is based on the work previously conducted by Ms. Grace van der Gugten and Dr. Mari DeMarco, which lays the groundwork for the Aims pursued in this work. A subset of the experiments in chapter 3 were also supported by the efforts of Ms. van der Gugten.

# Table of Contents

<b>Abstract.....</b>	<b>iii</b>
<b>Lay Summary.....</b>	<b>v</b>
<b>Preface.....</b>	<b>vi</b>
<b>Table of Contents.....</b>	<b>vii</b>
<b>List of Tables.....</b>	<b>x</b>
<b>List of Figures .....</b>	<b>xi</b>
<b>List of Abbreviations .....</b>	<b>xiii</b>
<b>Acknowledgements .....</b>	<b>xv</b>
<b>Chapter 1: Introduction .....</b>	<b>1</b>
1.1 Neuropathology.....	1
1.2 Amyloid Precursor Protein Metabolism .....	2
1.3 Amyloid Cascade Hypothesis .....	3
1.4 Types of AD.....	4
1.5 Diagnosis .....	5
1.5.1 Post-mortem Diagnosis.....	5
1.5.2 Antemortem Diagnosis .....	6
1.5.3 Imaging Biomarkers .....	6
1.5.4 CSF Biomarkers.....	7
1.6 Analytical Approaches for Quantification of A $\beta$ .....	9
1.6.1 Ligand Binding Methods .....	9

vii

1.6.2	Mass Spectrometry .....	9
1.7	Disease Modifying Therapeutics.....	10
1.8	Aims and Hypotheses.....	12
<b>Chapter 2: Pre-Analytical and Analytical Considerations for Quantification of A<math>\beta</math>40 and A<math>\beta</math>42</b>		
<b>by Mass Spectrometry .....</b>		<b>13</b>
2.1	Introduction.....	13
2.2	Methods .....	14
2.2.1	Samples.....	14
2.2.2	Surrogate Matrix .....	15
2.2.2.1	Statistical Analysis.....	15
2.2.3	Total Protein Matrix .....	15
2.2.4	Hemolysis Interference.....	16
2.2.5	Anti-Amyloid Therapeutics .....	16
2.3	Results .....	16
2.3.1	Surrogate Matrix .....	16
2.3.2	Total Protein Matrix .....	17
2.3.3	Hemolysis Interference.....	19
2.3.4	Anti-Amyloid Therapeutics .....	21
2.4	Discussion.....	24
2.5	Conclusion.....	26
<b>Chapter 3: Identification Autosomal Dominant Variants and Wild-type Amyloid-<math>\beta</math> Peptides in</b>		
<b>Cerebrospinal Fluid as a Novel Diagnostic Approach for Autosomal Dominant AD.....</b>		<b>27</b>
3.1	Introduction.....	27
3.2	Methods .....	28
3.2.1	Variants Within the A $\beta$ 42 Sequence .....	28
3.2.2	Heterozygous A $\beta$ Samples.....	28



3.3	Results .....	29
3.3.1	Variants Within the A $\beta$ 42 Sequence .....	29
3.3.2	Heterozygous A $\beta$ Samples.....	35
3.4	Discussion.....	39
3.5	Conclusion .....	39
<b>Chapter 4: Summary .....</b>		<b>41</b>
<b>References .....</b>		<b>42</b>

## List of Tables

Table 1: AD diagnostic classification system using biomarker profiles (adapted from C.R Jack Jr. <i>et al.</i> 2018).....	8
Table 2: Calculated % bias for total protein interference study. ....	19
Table 3: Effect of hemolysate on accuracy of A $\beta$ quantitation, as compared to a sample with no hemolysate contamination by visual inspection.....	21
Table 4: Calculated % bias for samples containing the 4g8 antibody. ....	23
Table 5: Calculated % bias for samples containing IVIG.....	23
Table 6. Published variants within the A $\beta$ 42 sequence. ....	30
Table 7. MRM transitions of wt-A $\beta$ 40, wt-A $\beta$ 42, the ISs and the A $\beta$ 40 variants meeting the selection criteria for MRM development.....	34

## List of Figures

Figure 1: APP processing showing the non-amyloidogenic pathway on the left and the amyloidogenic pathway on the right. ....	2
Figure 2: APP annotated with sequence variants associated with autosomal dominant AD occurring within the A $\beta$ 42 sequence. ....	5
Figure 3: Automated multiplex A $\beta$ LC-MS/MS assay workflow. ....	14
Figure 4: The optimal concentration for the surrogate matrix is between 0.5 – 2 g/L BSA. Average peak area for A) A $\beta$ 40 and B) A $\beta$ 42 over total protein concentration (g/L), represented as the mean of three technical replicates and the standard deviation. NS: Not significant. ....	17
Figure 5: Total protein concentration affects raw peak area signal but not quantification of A $\beta$ peptides. Average peak area and average A $\beta$ concentration versus total protein concentration (g/L), represented as the mean of three technical replicates and the standard deviation. A and B) A $\beta$ 40 and C and D) A $\beta$ 42. NI: No interference. ....	18
Figure 6: Hemolysate contamination affects raw peak area signal, but not quantification of A $\beta$ peptides. Peak area adjusted for endogenous A $\beta$ and A $\beta$ concentration is shown for each individual sample tested, represented as the mean of three technical replicates and the standard deviation. A) and B) A $\beta$ 40. C) and D) A $\beta$ 42. Hemoglobin contamination, but not necessarily total hemolysate contamination, increased from patient sample 0 to 4 as observed visually. The control sample contained no hemolysate by visual inspection. NI: No interference. ....	20
Figure 7: Presence of immunoglobulins do not interfere with the LC-MS/MS method. Average peak area (adjusted for endogenous A $\beta$ ) and A $\beta$ concentration for the control, 4g8 and IVIG samples, represented as the mean of three technical replicates and the standard deviation. A and B) A $\beta$ 40. C and D) A $\beta$ 42. The control sample was CSF pool with no 4g8 antibody and IVIG. NI: No interference. ....	23

Figure 8: Wt-A $\beta$  peak and E22G variant can be distinguished based on mass and retention time.

Chromatograms of pure solutions of A) wt-A $\beta$ 40 and B) E22G variant. MRMs of the heterozygote CSF sample showing the (C) wt-A $\beta$ 40 MRM and the (D) E22G variant MRM, where the semi-transparent boxes indicate the retention time window considered for peak detection. ....36

Figure 9: The variant E22Q was resolved chromatographically from wt-A $\beta$ . Chromatograms of

pure solutions of A) wt-A $\beta$ 40 and B) E22Q variant. MRMs of the heterozygote CSF sample showing the (C) wt-A $\beta$ 40 MRM and (D) E22Q variant MRM, where the semi-transparent boxes indicate the retention time window considered for peak detection.....37

Figure 10: LC-MS/MS chromatograms of wt-A $\beta$ 40 (blue) and AD autosomal dominant variants

(grey). A) Wt-A $\beta$ 40, B) Arctic (E22G), C) Dutch (E22Q), D) English (H6R), E) Flemish (A21G), F) Iowa (D23N), G) Italian (E22K), H) Osaka (E22 $\Delta$ ), I) Piedmont (L34V), J) Tottori (D7N). The semi-transparent boxes indicate the retention time window considered for peak detection. ....38

## List of Abbreviations

Alzheimer's disease (AD)

amyloid- $\beta$  ( $A\beta$ )

amyloid- $\beta$  1-40 sequence ( $A\beta$ 40)

amyloid- $\beta$  1-42 sequence ( $A\beta$ 42)

amyloid precursor protein (*APP*)

cerebrospinal fluid (CSF)

presenilin-1 (*PSEN1*)

presenilin-2 (*PSEN2*)

beta-site amyloid precursor protein-cleaving enzyme 1 (BACE)

soluble ectodomain known (sAPP $\beta$ )

carboxy-terminal fragment (CTF $\beta$ )

*APP* intracellular domain (AICD)

blood brain barrier (BBB)

Diagnostic and Statistical Manual of Mental Disorders, 4<sup>th</sup> edition (DSM-IV)

National Institute of Neurologic, Communicative Disorders and Stroke-AD and Related Disorders Association (NINCDS-ADRDA)

National Institute of Aging and the Reagan Institute (NIA-RI)

Consortium to Establish a Registry for Alzheimer Disease (CERAD)

International Working Group (IWG)

positron emission tomography (PET)

total-tau (t-tau)

phosphorylated tau (p-tau)

National Institute on Aging and Alzheimer's Association (NIA-AA)

mild cognitive impairment (MCI)

magnetic resonance imaging (MRI)

<sup>11</sup>C-Pittsburgh Compound-B (PIB)

enzyme-linked immunosorbent assay (ELISA)

liquid chromatography tandem mass spectrometry (LC-MS/MS)

mass spectrometry (MS)

solid phase extraction (SPE)

multiple reaction monitoring (MRM)

mass to charge ratio (m/z)

internal standard (IS)

wild-type (wt)

intravenous immunoglobulins (IVIG)

## **Acknowledgements**

I would like to thank my supervisor Mari DeMarco for having me as a master student and giving me the opportunity to work on this project.

My lab members, Serena Singh, Junyan Shi, Lauren Forgrave, and Taylor Pobran for their continuous support throughout this project.

My committee members, Honglin Luo, Philipp Lange, Haakon Nygaard, for their outstanding knowledge, enthusiasm and guidance during my master thesis.

# Chapter 1: Introduction

## 1.1 Neuropathology

Alzheimer's disease (AD) affects 50 million worldwide and accounts for the majority of all cases of dementia [1]. In 1906, Dr. Alois Alzheimer, who the disease was named after, characterized the abnormal deposits found in brains of individuals with cognitive impairment [2]. These abnormal deposits were identified to be extracellular plaques and intracellular neurofibrillary tangles which are the neuropathological hallmarks of AD [3]. The accumulation of plaques and neurofibrillary tangles lead to synaptic loss, plasticity changes, neuronal loss and eventually neurodegeneration [4]. In 1984, Dr. George Glenner and Dr. Cai'ne Wong identified amyloid- $\beta$  ( $A\beta$ ) the primary component of the extracellular plaques [5]. Soon after in 1986, researchers discovered that the neurofibrillary tangles found in AD were made of tau, a type of protein that stabilizes microtubules and gets released upon neurodegeneration [6, 7]. Abnormal hyperphosphorylation of tau results in formation of the neurofibrillary tangles.

$A\beta$  peptides are derived via proteolytic cleavage of the trans-membrane amyloid-precursor protein (APP) by endogenous proteases, resulting in peptides of various lengths, including residues 1-40 and 1-42, referred to herein as  $A\beta$ 40 and  $A\beta$ 42, respectively [8-10] (Figure 1). The plaques consist of fibrillar  $A\beta$ 42 formed via aggregation peptide monomers into higher order aggregates [11]. There is still debate on which forms of  $A\beta$  are the most neurotoxic; however, soluble smaller-order aggregates of  $A\beta$  have shown to be correlated with synapse loss and neuronal injury [12, 13], while  $A\beta$  fibrils have been shown to induce neuronal loss [11].



A $\beta$  being secreted into cerebrospinal fluid (CSF) was first reported in 1992, which made CSF an important candidate biomarker for AD [14]. Measurement A $\beta$ 40 and A $\beta$ 42 peptides along with tau protein and the phosphorylated form of tau have been proven to be reliable biochemical indicators of AD with a sensitivity and specificity of 85% and 95%, respectively [15].

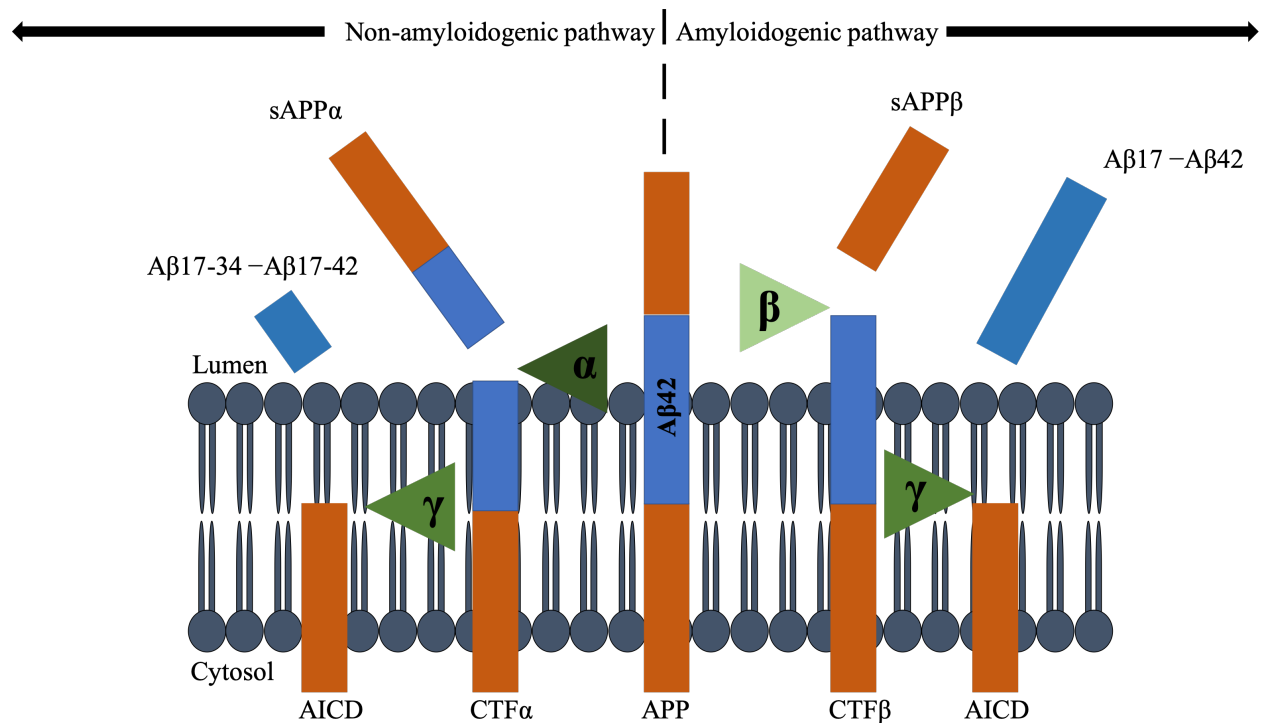


Figure 1: APP processing showing the non-amyloidogenic pathway on the left and the amyloidogenic pathway on the right.

## 1.2 Amyloid Precursor Protein Metabolism

APP can be processed and cleaved by several pathways producing A $\beta$  peptides that vary in length. Following the amyloidogenic pathway (Figure 1), APP is cleaved by  $\beta$ -secretase ( $\beta$ -site amyloid precursor protein-cleaving enzyme 1, BACE), which results in the release of the large

soluble ectodomain known as sAPP $\beta$ . The remaining carboxy-terminal fragment (CTF $\beta$ ) is then cleaved within the membrane-bound domain by  $\gamma$ -secretase, a complex consisting of at least four subunits: the enzymatic portion of the complex, presenilin 1 protein, presenilin 2 protein, presenilin enhancer 2; nicastrin; and anterior pharynx defective-1 [8, 10, 16-19], releasing the A $\beta$ 42 [20] and several carboxy-terminal truncated forms including A $\beta$ 40 and A $\beta$ 38 [9, 21] outside the cell and the APP intracellular domain into the cytoplasm. The function of APP and A $\beta$  remains unclear; however, it is known that the extracellular domain of the protease nexin form of APP is part of the clotting cascade [22], and it has been speculated to bind to other proteins on the surface of cells or help cells attach to one another [23]. Additionally, studies have suggested that APP helps to direct the migration of neurons during early development in the brain [23-26].

APP can also be cleaved following the non-amyloidogenic pathway, whereby cleavage is initiated by  $\alpha$ -secretase, which cuts APP at the luminal domain releasing an extracellular sAPP $\alpha$  domain and leaving the carboxyl-terminal fragment, CTF $\alpha$  in the plasma membrane, which can be further cleaved by  $\gamma$ -secretase. The non-amyloidogenic processing results in the generation of N-terminally truncated A $\beta$  peptides referred to as p3 peptides. The non-amyloidogenic processing pathway of APP, however, does not result in A $\beta$  generation.

### **1.3 Amyloid Cascade Hypothesis**

The central hypothesis for the development of AD is the amyloid cascade hypothesis, which states that an imbalance between the production and clearance of A $\beta$  causes plaque accumulation in the brain and is the initiating event, ultimately leading to neuronal degeneration and dementia

[2, 27-29]. There have been several clearance mechanisms for A $\beta$  that have been proposed such as enzymatic/proteolytic degradation, low-density lipoprotein receptor related clearance, clearance by cellular signaling pathways, and transport over the blood brain barrier (BBB) from CSF to blood. The proteolytic degradation of A $\beta$  is a major route of clearance.

While the amyloid cascade hypothesis remains the central hypothesis in AD, there is continuing debate about the exact role of amyloid in disease as there are findings that undercut its importance in pathogenesis. For example, the amyloid plaque burden does not correlate well with the degree of cognitive impairment when compared to neurofibrillary tangle count suggesting tangles may precede amyloid plaques [30]. Along the same lines, abundant amyloid plaques have been noted in individuals with no cognitive impairment [30]. These findings and the high number of failed clinical drug trials involved in targeting A $\beta$  emboldened critics of the amyloid cascade hypothesis; hindering its universal acceptance [31].

#### **1.4 Types of AD**

AD can be broadly divided into two types, sporadic or autosomal dominant. Sporadic AD accounts for the majority of the AD cases and typically first presents in those older than 65 years [2]. Autosomal dominant AD, accounts for less than 1% of all cases in those under 65 years of age. Autosomal dominant AD is caused by rare and highly penetrant dominantly inherited mutations referred to herein as autosomal dominant variants, in the *APP*, presenilin-1 (*PSEN1*) and presenilin-2 (*PSEN2*) genes [32-38]. Mutations in *PSEN1* account for 70% of autosomal dominant AD cases while mutations in *PSEN2* and *APP* are very rare among autosomal dominant AD cases [32, 33, 35, 39]. Mutations in *APP*, *PSEN1* and *PSEN2* genes have all been

shown to affect APP processing by altering the amounts and/or length of the A $\beta$  peptide produced [35, 40-42]. Diagnosis of autosomal dominant AD is confirmed by the identification of an autosomal dominant variant. Variants in APP, more specifically in the A $\beta$ 42 sequence, were investigated as part of this thesis (Figure 2).

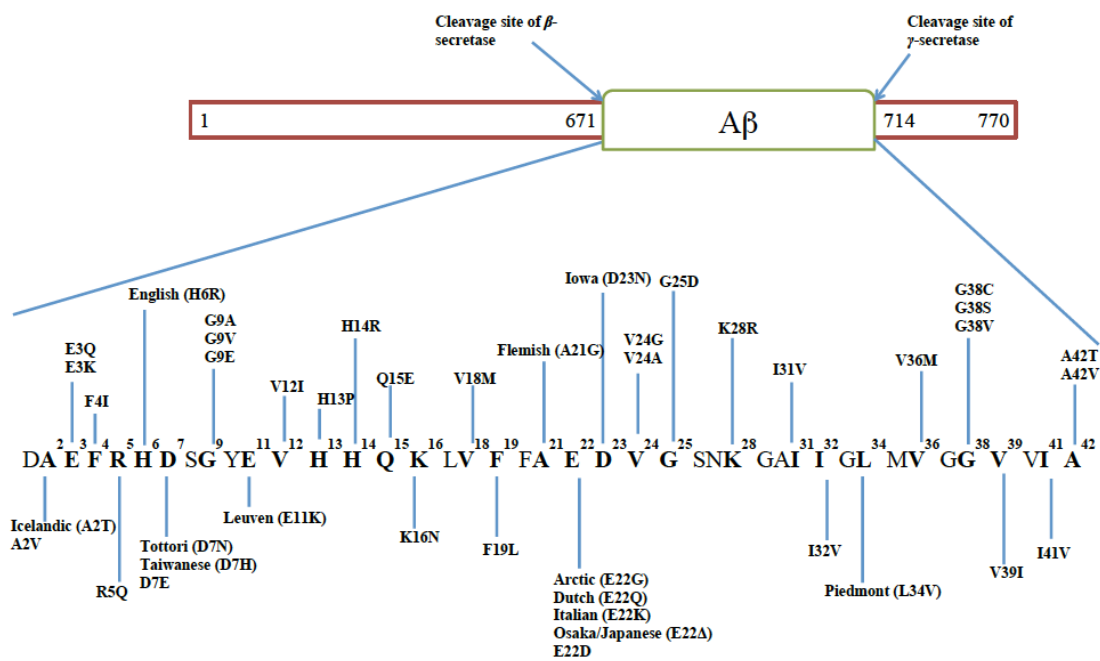


Figure 2: APP annotated with sequence variants associated with autosomal dominant AD occurring within the A $\beta$ 42 sequence.

## 1.5 Diagnosis

### 1.5.1 Post-mortem Diagnosis

To make a definitive AD diagnosis, the gold standard is identification of amyloid plaques and neurofibrillary tangles on post-mortem neuropathological examination. The recommendations of the National Institute of Aging and the Reagan Institute (NIA-RI) [43] for the neuropathological assessment for AD is to combine the Consortium to Establish a Registry for Alzheimer Disease

(CERAD) score of neuritic plaques [44] with the topographic staging of neurofibrillary tangles [45]. These criteria are divided into three categories: low, intermediate and high likelihood of AD, and a diagnosis of AD is made when the criteria for intermediate or high likelihood of AD are met and the individual had a clinical history of dementia [43].

### **1.5.2 Antemortem Diagnosis**

Antemortem diagnosis of AD is based on medical and family history, physical exam, neurological exam, mental status tests, diagnostic tests, and brain imaging [46]. The most widely used sets of criteria for diagnosis of AD are the Diagnostic and Statistical Manual of Mental Disorders, 5<sup>th</sup> edition (DSM-V) [47] and National Institute of Neurologic, Communicative Disorders and Stroke-AD and Related Disorders Association (NINCDS-ADRDA) [48, 49]. The NINCDS-ADRDA and DSM-IV criteria both have a sensitivity of 81% and specificity of 70% for clinical diagnosis of AD [46].

In support of improving diagnostic accuracy, CSF biomarkers have been incorporated into the diagnostic criteria of AD for research in the International Working Group guidelines, National Institute of Aging, and Alzheimer's Association (NIA-AA) Research Framework and in the Canadian Consensus Conference on Diagnosis and Treatment of Dementia [43, 50, 51], which are discussed further in section 1.5.4.

### **1.5.3 Imaging Biomarkers**

PET imaging, using tracers targeting the pathological protein aggregates, is one biomarker approach to detecting AD pathology [52]. The PET imaging of amyloid related

neuropathological changes associated with AD is performed using tracers such as  $^{11}\text{C}$ -Pittsburgh Compound-B (PIB) or  $^{18}\text{F}$ -labeled tracers such as flutemetamol [53-56]. These tracers enable visualization of the location of the deposits within the brain and can provide quantitative information on amyloid deposits [53, 57]. PET tracers for tau have only been recently tested in human trials, which include phenyl/pyridinyl-butadienyl benzothiazoles/benzothiazoliums [58] and 18F-T808 [59]. Limitation of the use of PET imaging in routine care is the short half-life of these tracers, which presents challenges in availability, require an on-site cyclotron, radiochemistry expertise, and is an expensive test [52, 60].

#### **1.5.4 CSF Biomarkers**

In addition to imaging biomarker, biofluid marker can also be used to assess the presence of AD neuropathology via quantitation of A $\beta$  peptides and tau in CSF [52]. More specifically, the concentration of A $\beta$ 42 in CSF has been proven to be a reliable biomarker for AD with the concentration of A $\beta$ 42 being ~50% lower in individuals with AD compared to healthy controls [61]. Notably, changes in the concentration of A $\beta$ 42 in CSF precede changes observed via PET imaging as observed in multiple studies involving individuals with AD [55, 56, 62, 63].

The NIA-AA Research Framework defines AD by its underlying pathologic processes that can be documented by post-mortem examination or *in vivo* using biomarkers [43]. The NIA-AA Research Framework proposed the AT(N) biomarker classification system for the symptomatic or “clinical” stages of AD, that is, mild cognitive impairment (MCI) and dementia [43]. The “A” in the biomarker classification system represents CSF A $\beta$  peptides and cortical amyloid PET ligand binding. The “T” biomarkers represent the neurofibrillary tangles and are measured via

CSF p-tau or cortical tau PET ligand binding. Biomarkers of neurodegeneration or neuronal injury (labeled “N”) are measured using CSF t-tau, FDG PET hypometabolism or observation of atrophy on magnetic resonance imaging (MRI) [43]. Structural and functional MRI is used to support clinical AD diagnosis. Structural MRI visualized the cerebral atrophy characteristics for neurodegeneration [64-67]. Functional MRI measures activity within the brain by using blood-oxygen-level dependent contrast imaging [68, 69] to study functional connectivity and detect early brain dysfunction related to AD. In this classification system, the three biomarker groups are profiled as positive (+, abnormal) or negative (–, normal) and are then grouped accordingly into three possible biomarker categories (Table 1).

Table 1: AD diagnostic classification system using biomarker profiles (adapted from C.R Jack Jr. *et al.* 2018).

A	T	(N)	Interpretation	
–	–	–	Normal Alzheimer’s disease biomarkers	
+	–	–	Alzheimer’s pathologic change	Alzheimer’s continuum
+	+	–	Alzheimer’s disease	
+	+	+	Alzheimer’s disease	
+	–	+	Alzheimer’s and concomitant suspected non-Alzheimer’s pathologic change	
–	+	–	Non-Alzheimer’s disease pathologic change	
–	–	+	Non-Alzheimer’s disease pathologic change	
–	+	+	Non-Alzheimer’s disease pathologic change	

## **1.6 Analytical Approaches for Quantification of A $\beta$**

### **1.6.1 Ligand Binding Methods**

Many different approaches have been used for quantification of A $\beta$  peptides including various ligand binding methods: enzyme-linked immunosorbent assay (ELISA), radioimmunoassay, biochip immunoassays, electrochemiluminescence, immunoelectrophoresis, and nephelometry [15, 70-74]. Immunoassays, in general, rely on the interaction between antibodies and the analyte of interest for quantification, providing an indirect measurement of antigen quantity.

Unfortunately, accuracy and precision can be affected by several factors including hemolysate, proteins, and therapeutic products [75-78]. Antibodies are also known to cross-react with substances other than the target analyte, potentially resulting in positive or negative interference [79, 80]. Additionally, immunoassays also cannot distinguish among modified and processed forms of the analyte of interest such as between the A $\beta$  autosomal dominant variants.

### **1.6.2 Mass Spectrometry**

Mass spectrometry (MS) is a technique that can address the many of the limitations of immunoassays and therefore has been increasingly used in clinical laboratories for absolute quantitation of peptides and proteins [81]. MS is a widely used analytical technique and is capable of providing information about the qualitative and quantitative composition of complex mixtures [82]. A central advantage of liquid chromatography tandem mass spectrometry (LC-MS/MS) is the exquisite analyte selectivity derived from the use of multiple reaction monitoring (MRM). LC is used to separate analytes in time, and MS/MS enables further selectivity by the analyte's mass-to-charge ( $m/z$ ) ratio and subsequent confirmation of the analyte's primary structure (i.e. sequence) by fragmentation. The use of MRM is akin to performing a sequencing



experiment for each analyte detected where the peptide (i.e. precursor ion) is reproducibly fragmented into a series of overlapping peptide sequences, and the fragment m/z ratios are then detected to confirm the identity of the target analyte. This level of selectivity, far exceeding that of immunoassays, is the reason the laboratory medicine community has turned to MS for the development of reference methods (i.e. gold standard methods) and for quantification of clinically relevant peptide and proteins [70-74, 83], including a candidate reference method for A $\beta$  [84]. MS being able to differentiate between A $\beta$  isoforms can thus provide accurate quantification of total A $\beta$ . Additionally, an MRM method allows for screening of multiple analytes in a single analysis, increasing the multiplexing capacity of the method when compared to immunoassays.

Quantification is achieved by mixing a known amount of isotope-labelled (e.g.,  $^{15}\text{N}$  or  $^{13}\text{C}$  labelled) internal standard (IS) peptide with the sample. The ideal IS is one that is chemically equivalent to the endogenous peptide – such as an isotopically labelled version of the measured analyte – where it behaves in a similar fashion throughout the entire analytical process: sample preparation, chromatography, ionization, fragmentation and detection. The resulting LC-MS/MS peak area ratio of the endogenous peptide measured to that of its IS is then used for comparison to an external calibration curve for quantification.

## **1.7 Disease Modifying Therapeutics**

There are several symptomatic therapies for AD; however, no disease-modifying therapies are currently available. A major focus of development of therapeutics for AD is on therapeutic monoclonal antibodies targeting A $\beta$  and/or A $\beta$  aggregates. In active immunotherapy, the

individual's immune system is activated to remove A $\beta$  peptides to reduce the formation of amyloid plaques. Active immunotherapy (or A $\beta$  vaccination) involves activation of the individual's immune system to stimulate the production of endogenous anti-A $\beta$  antibodies [85]. These antibodies bind to the A $\beta$  peptides and are cleared out the brain. Passive immunotherapy administers exogenous monoclonal antibodies by infusion of humanized or human anti-A $\beta$  antibodies produced in the laboratory to clear A $\beta$  peptides and plaques [85]. An advantage of passive immunotherapy is being able to control adverse events by manually stopping treatments. Current passive immunotherapeutic approaches for AD require improvement with efficiency of the antibody-A $\beta$  complex crossing the BBB (only approximately 0.1% cross the BBB) as well as the cross reactivity and the inflammatory alterations [86].

Despite the many promising therapeutic approaches, the clinical trials have failed to show positive effects on primary clinical outcome [85, 87]. This can be due to the drug treatments not being commenced early enough in the disease, before neurodegeneration is too severe and widespread [85]. In 2010, Clifford Jack proposed a hypothetical model of biomarkers of the AD pathological cascade [88]. The model relates disease stages to AD biomarkers where A $\beta$  biomarkers become abnormal first, then neurodegeneration biomarkers and cognitive symptoms, lastly neurodegenerative biomarkers, which correlate with clinical symptom severity. This model suggests that A $\beta$  biomarkers can be used to identify individuals in the pre-symptomatic phase of AD for clinical trial enrolment. If treatment can be initiated at an earlier stage of the disease, before neurodegeneration is too severe, it may give promising drug candidates a chance of showing a disease-modifying effect. Additionally the diagnostic procedure in enrolling individuals for clinical trials needs refinement so that only individuals designated as having AD

in the trial have objective evidence of AD pathology [85]. Thus, research on the development of more specific and accurate diagnostic tools, specifically A $\beta$  CSF diagnostic test, are important for patient enrichment at earlier stages of the disease.

## **1.8 Aims and Hypotheses**

The aims of this thesis were to improve the diagnostic power of CSF biomarker testing for AD by optimizing/modifying the laboratory's existing quantitative wt-A $\beta$  LC-MS/MS method.

Hypotheses tested pertaining to the LC-MS/MS A $\beta$  method were as follows:

1. By assessing analytical performance characteristics of the LC-MS/MS method in the presence of potential interferents, criteria for sample acceptance/rejection can be developed for use in routine care.
2. If modifications are made to the quantitative wt-A $\beta$  LC-MS/MS method, it can be adapted to also detect known A $\beta$  variants as a diagnostic tool for autosomal dominant AD.

## **Chapter 2: Pre-Analytical and Analytical Considerations for Quantification of A $\beta$ 40 and A $\beta$ 42 by Mass Spectrometry**

### **2.1 Introduction**

An automated A $\beta$  LC-MS/MS method to quantify and detect wt-A $\beta$  peptides was previously developed (Figure 3) [89]. The LC-MS/MS workflow is summarized as follows: 200  $\mu$ L of CSF aliquots were treated with guanidine HCl and the  $^{15}$ N-A $\beta$ 40 and  $^{15}$ N-A $\beta$ 42 IS added, followed by SPE by mixed-mode cation exchange, and followed by LC-MS/MS analysis on a Shimadzu high performance LC and SCIEX 5500 triple quadrupole mass spectrometer. This multiplex A $\beta$  LC-MS/MS assay was validated in a clinically accredited laboratory following Clinical and Laboratory Standards Institute guidelines including C62, EP-5A, and EP-6A [90-92].

The first aim of this thesis was to optimizing the assay by evaluating the pre-analytical and analytical factors that could effect accurate and precise quantification of the analytes of interest [75, 93]. Endogenous and exogenous factors looked at included hemolysate (to model a traumatic lumbar puncture), total protein, and immunoglobulins. With clinical implementation in mind, the outcomes of the work would be used to develop criteria for sample acceptance/rejection.

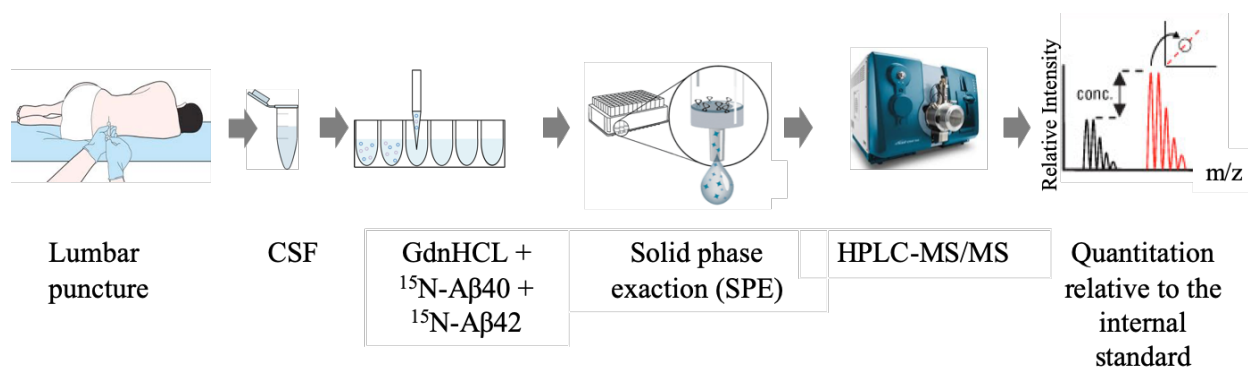


Figure 3: Automated multiplex Aβ LC-MS/MS assay workflow.

## 2.2 Methods

Spike and recovery experiments were performed to determine interference. Effect on Aβ quantitation was assessed as both the raw signal (peak area) and signal normalized by the internal standard (analyte concentration). Matrix interference is evaluated in the context of bias, which is the difference between the expected value and the measured value. In the interference studies performed, the expected value is the known concentration of Aβ peptides spiked into a sample. The pre-specified acceptance criteria for both Aβ40 and Aβ42 was a bias within  $\pm 20\%$  of the expected concentration.

### 2.2.1 Samples

For the spike and recovery experiments performed, pools of human CSF collected from patients at the St. Paul's Hospital in Vancouver, Canada, following an established protocol (REB# H18-03050) were used. All samples were analyzed using the multiplex Aβ LC-MS/MS assay (Figure 3).

### **2.2.2 Surrogate Matrix**

A spike and recovery experiment with bovine serum albumin (BSA) was used to determine the optimal range of total protein for the surrogate matrix used to make up the calibrators. Samples with concentrations of ranging from 0 to 20 g/L of BSA were prepared in phosphate buffered saline (PBS) and each sample was spiked with a final concentration of the following synthetic peptides: 15 ng/mL for A $\beta$ 40 and 1000 pg/mL for A $\beta$ 42. Samples were analyzed in triplicate using the LC-MS/MS method to identify the optimal range for A $\beta$  recovery.

#### **2.2.2.1 Statistical Analysis**

The Mann-Whitney test was used to compare peak area signal between different BSA concentrations. Statistical differences were noted if the calculated  $P < 0.05$ .

### **2.2.3 Total Protein Matrix**

A ‘high’ total protein CSF pool was created by pooling individual samples with high total protein concentration and spiking in plasma to create a pool with a concentration of ~10 g/L total protein. A ‘low’ total protein CSF pool was made by pooling individual samples with low total protein concentration. Using the ‘high’ and ‘low’ CSF pools, various mixed solutions were prepared with concentrations ranging from undetectable (i.e., less than the lower limit of the analytical measuring range of 0.01 g/L) to 10.0 g/L of total protein. Each sample was then spiked with synthetic A $\beta$  peptides to a final concentration of 20 ng/mL A $\beta$ 40 and 3 ng/mL A $\beta$ 42. Three technical replicates were run for each sample and analyzed by LC-MS/MS.

#### **2.2.4 Hemolysis Interference**

To test the visual cut off, a spike and recovery experiment was then performed using four human CSF samples with various concentrations of hemolysate contamination determined visually from its color and appearance. Each sample was then spiked with synthetic A $\beta$  peptides to a final concentration of 20 ng/mL A $\beta$ 40 and 3 ng/mL A $\beta$ 42. Three technical replicates were run for each sample and analyzed by LC-MS/MS. Percent bias was calculated by setting the sample with no hemolysate contamination by visual inspection as 100% recovery.

#### **2.2.5 Anti-Amyloid Therapeutics**

To mimic an anti-A $\beta$  monoclonal antibody therapeutic, an anti-A $\beta$  antibody (i.e., clone 4g8 an anti-A $\beta$  (17-24) mouse IgG monoclonal antibody) that binds to the same epitope as a known candidate therapeutic antibody (i.e., crenuzumab) was spiked into a CSF pool at concentrations ranging from 0.05 – 0.6 ng/mL [94]. As a control, intravenous immunoglobulin (IVIG) was also spiked into a CSF pool ranging from at 0.05 ng/mL to 0.6 ng/mL. A $\beta$ 42 and A $\beta$ 40 were spiked into the samples at 3 ng/mL and 20 ng/mL respectively. Samples were analyzed in triplicate by LC-MS/MS. Percent bias was calculated by setting the control sample, which was CSF pool with no immunoglobulins spiked in as 100% recovery.

### **2.3 Results**

#### **2.3.1 Surrogate Matrix**

Testing various concentrations of BSA indicated the optimal A $\beta$  recovery is between 0.5 – 2 g/L BSA. There was also no significant difference in A $\beta$  recovery between 0.5 – 2 g/L BSA.

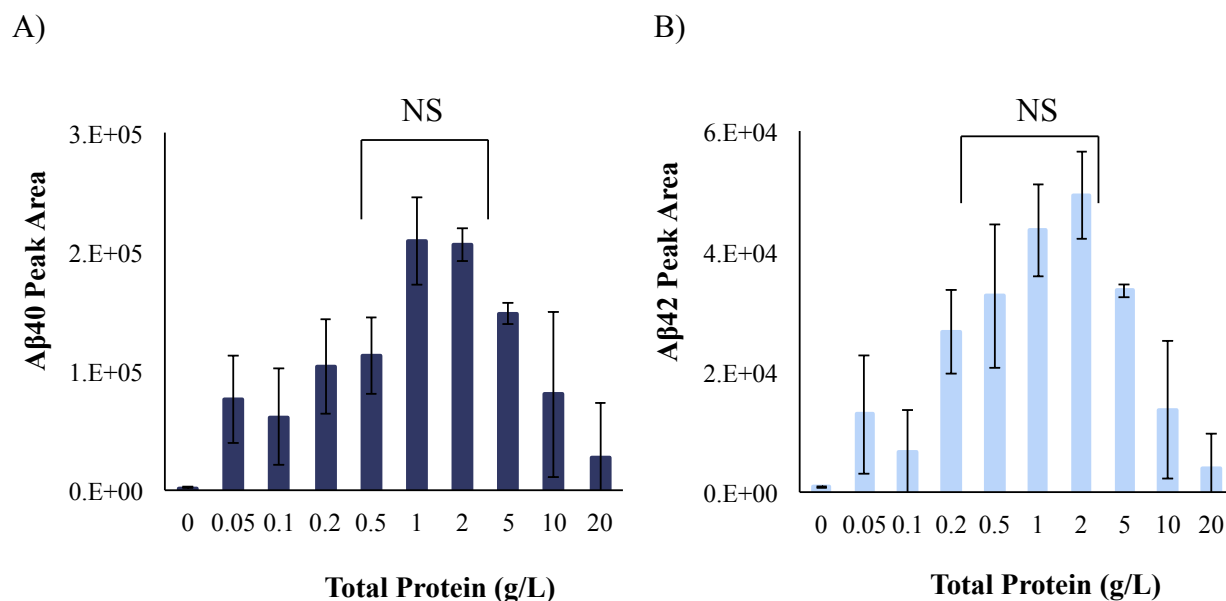


Figure 4: The optimal concentration for the surrogate matrix is between 0.5 – 2 g/L BSA.

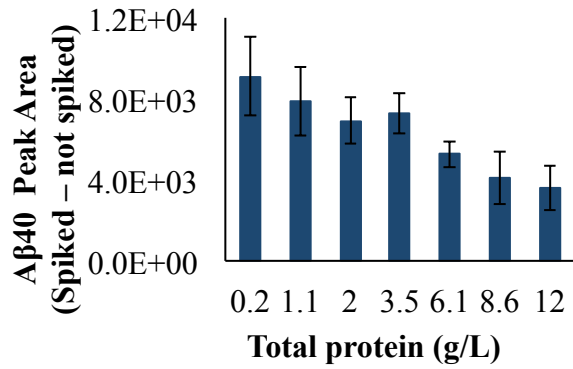
Average peak area for A) Aβ40 and B) Aβ42 over total protein concentration (g/L), represented as the mean of three technical replicates and the standard deviation. NS: Not significant.

### 2.3.2 Total Protein Matrix

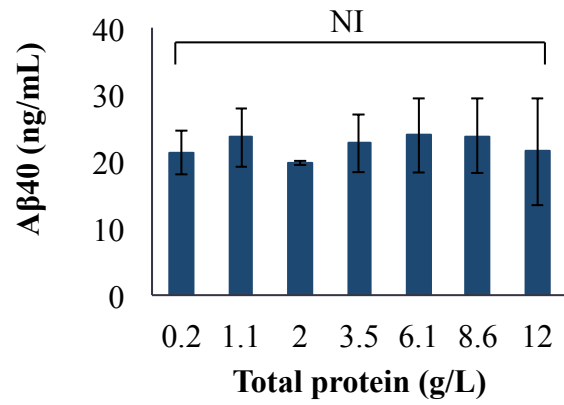
Peak area was inversely proportional to the total protein concentration over the range of 0.2 – 12 g/L; however, there was no effect on quantitation of Aβ (Figure 5) as recovery of Aβ for all samples was within  $\pm 20\%$  of the expected concentration (Table 2).



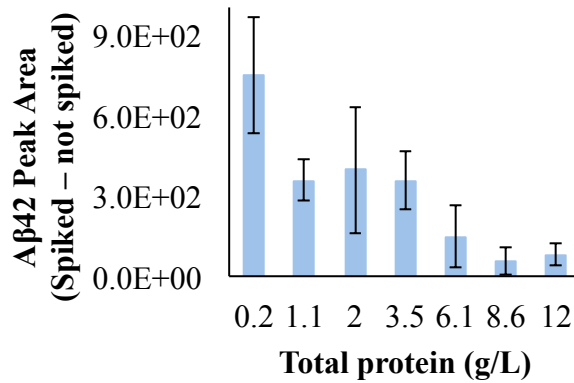
A)



B)



C)



D)

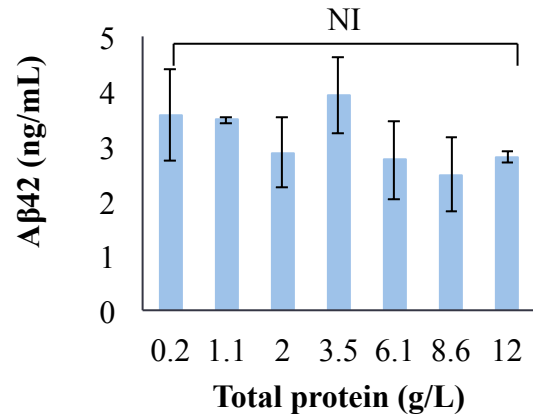


Figure 5: Total protein concentration affects raw peak area signal but not quantification of Aβ peptides. Average peak area and average Aβ concentration versus total protein concentration (g/L), represented as the mean of three technical replicates and the standard deviation. A and B) Aβ40 and C and D) Aβ42. NI: No interference.

Table 2: Calculated % bias for total protein interference study.

<b>Total protein (g/L)</b>	<b>A<math>\beta</math>42 % bias</b>	<b>A<math>\beta</math>40 % bias</b>
12.0	-6.8	7.5
8.6	-17.4	19.2
6.1	-8.5	19.5
3.5	13.0	13.5
2.0	-3.9	-1.6
1.1	15.7	18.1
0.2	18.6	6.4

### 2.3.3 Hemolysis Interference

There was variability in raw peak area signal between the hemolysate contaminated samples; however, there was no effect on quantitation of A $\beta$  (Figure 6) as the recovery of A $\beta$  for all hemolysate samples were within  $\pm 20\%$  of the expected concentration (Table 3).

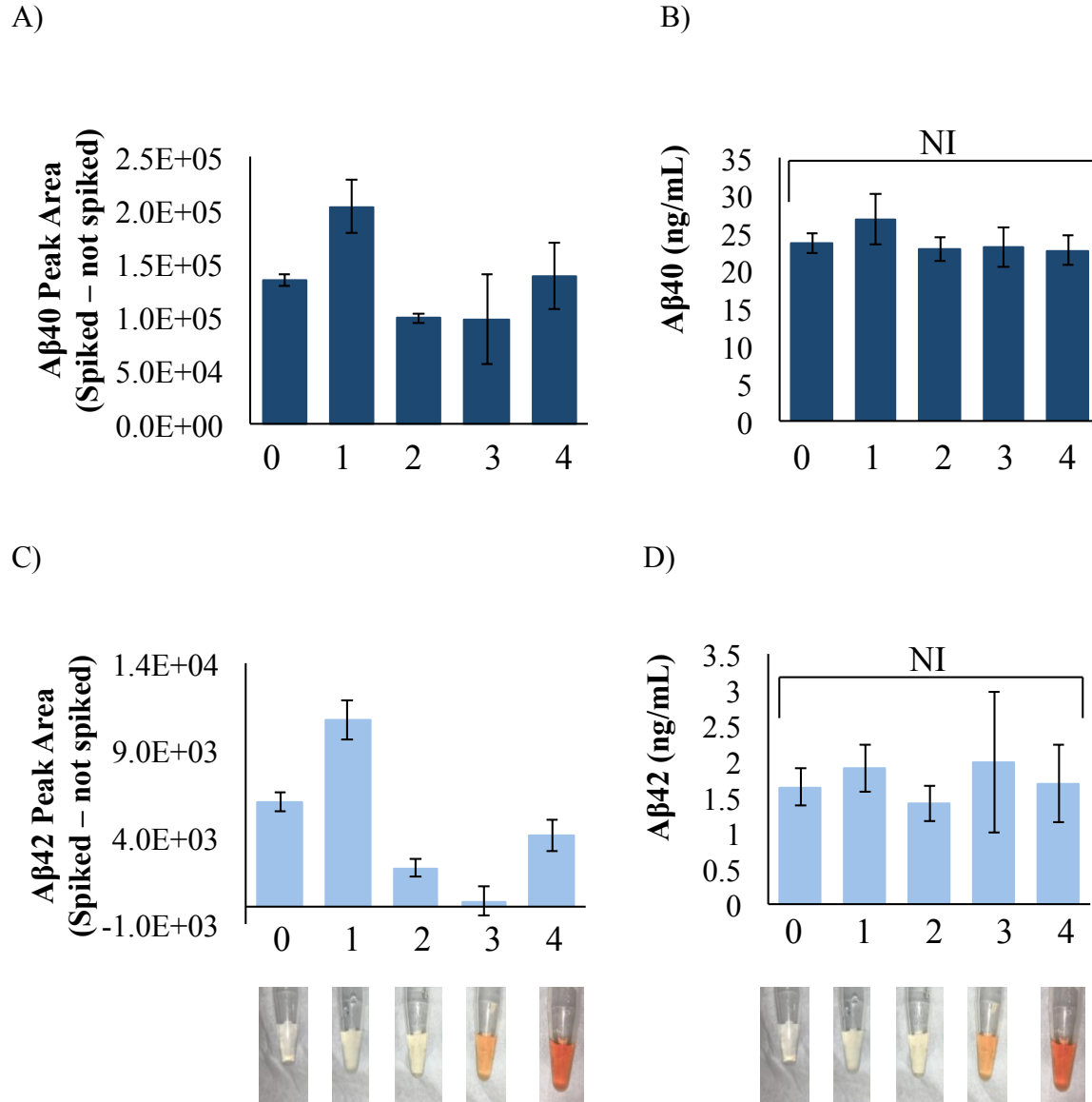


Figure 6: Hemolysate contamination affects raw peak area signal, but not quantification of Aβ peptides. Peak area adjusted for endogenous Aβ and Aβ concentration is shown for each individual sample tested, represented as the mean of three technical replicates and the standard deviation. A) and B) Aβ40. C) and D) Aβ42. Hemoglobin contamination, but not necessarily total hemolysate contamination, increased from patient sample 0 to 4 as observed visually. The control sample contained no hemolysate by visual inspection. NI: No interference.

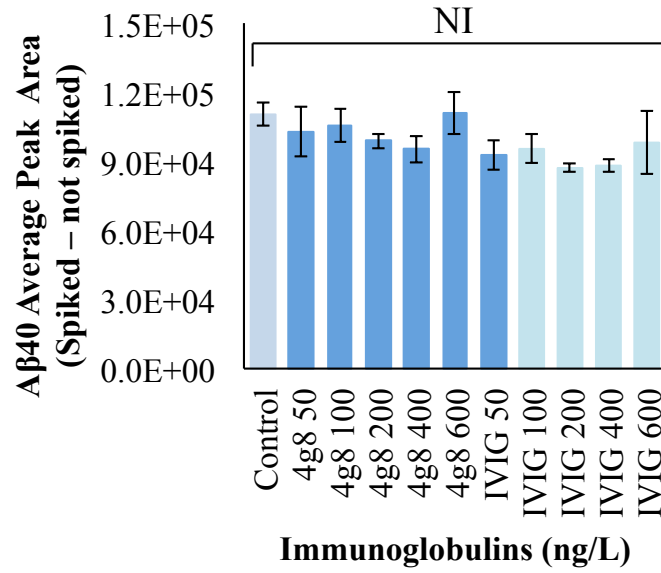
Table 3: Effect of hemolysate on accuracy of A $\beta$  quantitation, as compared to a sample with no hemolysate contamination by visual inspection.

Hemolysate Sample	A $\beta$ 42 % bias	A $\beta$ 40 % bias
1	15.1	13.9
2	-13.2	-3.5
3	19.9	-2.2
4	3.0	-3.8

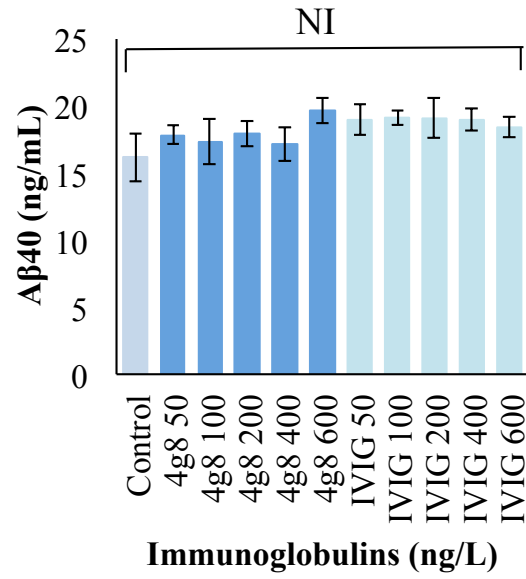
#### 2.3.4 Anti-Amyloid Therapeutics

There was no interference observed as all immunoglobulin samples tested were within the pre-specified acceptance criteria of  $\pm 20$  % bias for both A $\beta$ 40 and A $\beta$ 42 (Table 4 and 5). Figure 7 demonstrates the minimal differences in raw peak area signal and A $\beta$  concentration between the samples and the control (CSF pool).

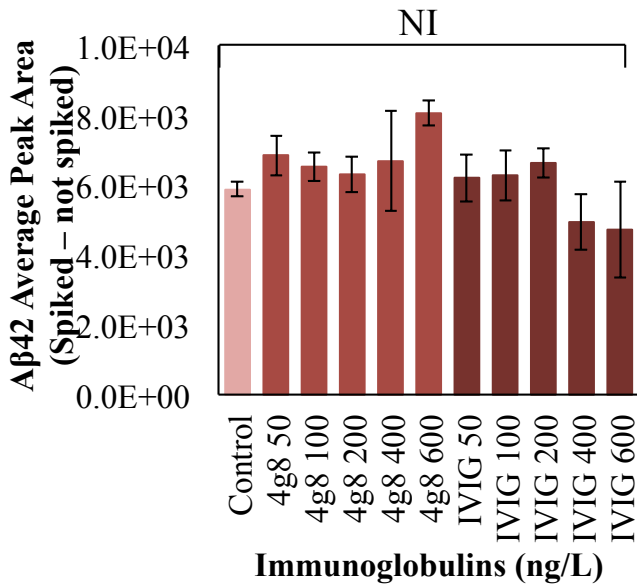
A)



B)



C)



D)

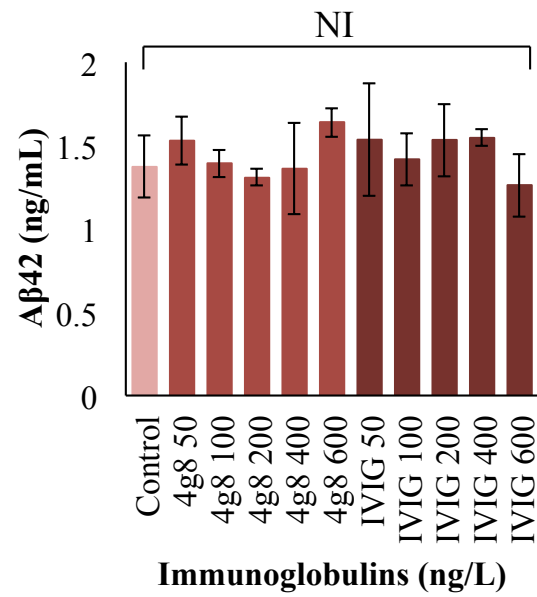


Figure 7: Presence of immunoglobulins do not interfere with the LC-MS/MS method. Average peak area (adjusted for endogenous A $\beta$ ) and A $\beta$  concentration for the control, 4g8 and IVIG samples, represented as the mean of three technical replicates and the standard deviation. A and B) A $\beta$ 40. C and D) A $\beta$ 42. The control sample was CSF pool with no 4g8 antibody and IVIG. NI: No interference.

Table 4: Calculated % bias for samples containing the 4g8 antibody.

<b>4g8 (ng/L)</b>	<b>A<math>\beta</math>42 % bias</b>	<b>A<math>\beta</math>40 % bias</b>
50	11.5	10.2
100	1.6	7.4
200	-4.8	10.9
400	-0.8	5.8
600	19.6	20.9

Table 5: Calculated % bias for samples containing IVIG.

<b>IVIG (ng/L)</b>	<b>A<math>\beta</math>42 % bias</b>	<b>A<math>\beta</math>40 % bias</b>
50	11.9	17.1
100	3.3	18.1
200	11.8	17.8
400	12.7	17.1
600	-8.0	13.6

## 2.4 Discussion

In a quantitative LC-MS/MS method, calibrators are made by spiking in a known amount of the analyte into the appropriate matrix. In the case of A $\beta$ , the matrix is CSF and as this already contains endogenous A $\beta$ , it is not ideal to then spike in synthetic A $\beta$ ; therefore, an alternate matrix must be sought. Commercially available synthetic CSF, termed ‘artificial CSF’ is an option; however, these solutions contain only buffering small molecules and ions, and no proteins. A $\beta$  peptides, in particular A $\beta$ 42, are hydrophobic and prone to aggregation, thus using artificial CSF with no proteins may lead to low recovery of the analyte [95]. Therefore, to better mimic CSF, an in-house surrogate matrix was designed for the LC-MS/MS calibrators. Testing various concentrations of BSA spiked into a buffered solution showed A $\beta$  recovery was optimal in the range of 0.5 – 2 g/L of total protein. The concentration of the surrogate matrix was set to 1 g/L total protein. This concentration was similar to the normal physiological range of total protein CSF, where the reference cut-point most commonly used is < 0.45 g/L and samples received in clinically laboratories typically fall in the range of 0.2 to 0.8 g/L of total protein for a population that excludes individuals with disorders that are known or suspected to increase CSF total protein [96].

Samples with endogenous total protein concentrations within and above the reference cut-point, were also tested to assess potential impact of total protein content on routine clinical samples which vary in total protein concentration. These analyses indicated that raw peak area signal decreased with increasing total protein concentration for both A $\beta$ 40 and A $\beta$ 42; however, quantification of both A $\beta$ 40 and A $\beta$ 42 was not affected by total protein concentration, due to

normalization by the IS. Thus, the LC-MS/MS method was not affected by physiologically plausible extremes in total protein concentration.

CSF samples containing hemolyzed red blood cells were also investigated, which can occur due to a traumatic lumbar puncture or leakage of the BBB. In routine clinical analysis, hemolysate contamination is judged based on color and appearance of the CSF sample. Real patient specimens with hemolysate contamination based on visual inspection were also evaluated to test for potential interference in the LC-MS/MS method. The results from this interference study indicated that raw signal was affected by the hemolysate contamination; however, A $\beta$  quantification was not affected as a result of the IS normalization process (i.e., use of ion peak area ratios of analyte/IS). From previous experiments performed in the laboratory, a visual cutoff for hemolysate contamination was determined, which visually corresponds to the color and appearance of patient sample 2 (Figure 6). The previous experiment performed used whole blood spiked into a CSF pool at various proportions; the solutions were then centrifuged and the supernatant analyzed. The color and appearance at this pre-determined visual cutoff is considered a physiologically plausible extreme for hemolysate contamination. In a clinical setting, in particular, out-patients being investigated for signs and symptoms of cognitive impairment, samples exceeding this amount of hemolysate contamination are unlikely.

In addition to potential endogenous interferents, plausible exogenous interferents, such as relevant therapeutic molecules, must be investigated as part of method validation [77]. In the context of AD, therapeutic molecules targeting A $\beta$  are of particular interest. While there are many anti-A $\beta$  antibody therapeutics under evaluation, they are not commercially available for purchase. As a surrogate, anti-A $\beta$  monoclonal antibody 4g8 was purchased for testing. 4g8 binds



residues 18-22 of A $\beta$ , sharing the same epitope with crenezumab, a passive immunotherapy that uses monoclonal antibodies to target multiple forms of aggregated A $\beta$  [94]. IVIG was used as a non-A $\beta$ -specific polyclonal antibody source. In the analyses, neither 4g8 or IVIG affected raw signal nor quantitation of A $\beta$  by LC-MS/MS; suggesting that the assay was not susceptible to anti-A $\beta$  therapies and the method can be used for not only in routine care, but also in clinical trials for anti-A $\beta$  therapeutics. It was anticipated that anti-A $\beta$  therapeutics would not interfere in the LC-MS/MS method due to the assay workflow, which includes, for instance, incubation with a strong salt denaturant (i.e., 5 M GdnHCl). For confirmation, the interference studied performed herein, can be directly applied to the investigation of other anti-A $\beta$  therapeutics.

## **2.5 Conclusion**

Pre-analytical and analytical steps of the LC-MS/MS method were optimized by identifying the optimal surrogate matrix concentration as well as by investigating potential interference. The surrogate matrix was established with protein content comparable to that observed in human CSF. Quantification of A $\beta$ 40 and A $\beta$ 42 was not affected by differences in total protein concentration. No interference from hemolysate was observed within the range of physiologically plausible contamination tested. Additionally, the presence of either non-specific or anti-A $\beta$  immunoglobulins did not affect raw signal or quantification of A $\beta$  peptides by LC-MS/MS. Thus A $\beta$  peptides can be accurately quantified in the presence of high total protein concentration and anti-A $\beta$  therapeutic antibodies, enabling use in routine clinical care and clinical trials. From the studies performed, pre-analytical requirements and sample acceptance/rejection criteria for the LC-MS/MS method were established.

## **Chapter 3: Identification Autosomal Dominant Variants and Wild-type Amyloid- $\beta$ Peptides in Cerebrospinal Fluid as a Novel Diagnostic Approach for Autosomal Dominant AD**

### **3.1 Introduction**

Currently published mass spectrometric methods do not include MRMs of known autosomal dominant A $\beta$  variants [70-74] and due to the high analytical selectivity of the MRM approach, A $\beta$  variants are “invisible” (i.e. not detected). Immunoassays for their part cannot differentiate between A $\beta$  variants that occur outside of the assay epitope regions, or if the mutation does occur within the epitope region (e.g. H6R variant) it may abrogate binding/detection. The A $\beta$  variants will thus not be detected and will result in falsely low A $\beta$ . Therefore, a method that identifies A $\beta$  variants within the A $\beta$ 42 sequence addresses accurate quantification of total A $\beta$  and also enables confirmatory diagnosis of AD.

The second aim of this thesis was to adapt the automated multiplex LC-MS/MS assay previously developed in the laboratory to identify known autosomal dominant variants within the A $\beta$ 42 sequence in CSF (Figure 2) [89]. As mentioned previously, *APP* autosomal dominant variants are 100% penetrant and result in autosomal dominant AD. Thus, identification of these variants in CSF can identify autosomal dominant AD. As a proof of concept study, nine pathogenic variants found in the A $\beta$ 42 sequence were tested to determine whether they could be identified and distinguished from wt-A $\beta$ .

## **3.2 Methods**

### **3.2.1 Variants Within the A $\beta$ 42 Sequence**

To develop a comprehensive A $\beta$  LC-MS/MS method that included both wt-A $\beta$  and variant sequences, a list of known variants within the A $\beta$ 42 sequence was developed by searching existing databases including: Alzforum, Single Nucleotide Polymorphism Database (dbSNP, NCBI), Exome Aggregation Consortium (ExAC). An APP variant was included in the MRM method if it satisfied the following criteria: (1) contained a sequence variation within the A $\beta$ 42 sequence, and (2) was either identified as non-pathogenic or of unknown significance with an average frequency in the global population of  $\geq 4.0\text{E-}05$ , or was identified as pathogenic (average frequency not considered in this case).

### **3.2.2 Heterozygous A $\beta$ Samples**

To test the multiplex A $\beta$  LC-MS/MS method, CSF representative of this heterozygous A $\beta$  expression state was used for testing – consistent with genetic make-up of individuals with autosomal dominant AD due to mutations in *APP*, who carry a single variant *APP* allele. As proof-of-concept, nine of these variants were synthesized as A $\beta$ 40 peptides and used to create the representative autosomal dominant AD CSF samples. No known pathogenic variants resulted in a mutation to residues 41 or 42, therefore all variants were captured within the A $\beta$ 40 sequence. To create a series of CSF samples characteristic of this heterozygote state, synthetic A $\beta$ 40 variants were spiked into a human CSF pool (containing only wt-A $\beta$ ) at equimolar concentration to the endogenous wt-A $\beta$ 40 (0.157 nM). An MRM method was developed for

these nine variants using MS. A predictive software, Skyline [97] was then used to build an MRM method with the remaining variants meeting the inclusion criteria be included in the adapted multiplex LC-MS/MS assay. Samples were then analyzed using the LC-MS/MS method shown in Figure 3. MRM peaks were considered within a retention time window of  $\pm 0.2$  minutes of the expected peak.

### **3.3 Results**

#### **3.3.1 Variants Within the A $\beta$ 42 Sequence**

Table 6 lists all variants in the A $\beta$ 42 region, phenotype (if reported), relevant disease (i.e., AD, cerebral amyloid angiopathy [CAA] and/or Parkinson's Disease Dementia [PDD]) and the global population frequency from Database searches (Genome Aggregation Database (GnomAD-Exomes), Trans-Omics for Precision Medicine (TOPMed), Exome Aggregation Consortium (ExAC), and the NHLBI GO Exome Sequencing Project (GO-ESP) Exome Variant Server.

Table 6. Published variants within the A $\beta$ 42 sequence.

Variant	Phenotype	Disease Relevance	Frequency				Average Frequency
			GnomAD-Exomes	TOPMED	ExAC	GO-ESP	
<b>Icelandic (A2T)</b>	Protective	AD	4.6E-04	1.1E-04	4.7E-04	1.0E-04	4.6E-04
<b>A2V</b>	Pathogenic	AD					
<b>E3Q</b>	Unknown		4.0E-05	2.0E-05	1.0E-05		2.3E-05
<b>E3K</b>	Unknown		4.0E-05	2.0E-05	1.0E-05		2.3E-05
<b>F4I</b>	Unknown				1.0E-05		1.0E-05
<b>R5Q</b>	Unknown		2.0E-05	3.0E-05	4.0E-05		3.0E-05
<b>English (H6R)</b>	Pathogenic	AD	1.0E-05				1.0E-05
<b>Taiwanese (D7H)</b>	Pathogenic (AD)	AD					
<b>Tottori (D7N)</b>	Pathogenic (AD)	AD					
<b>D7E</b>	Unknown			1.0E-05			1.0E-05
<b>G9A</b>	Unknown			1.0E-05	1.0E-05	1.0E-04	4.0E-05
<b>G9V</b>	Unknown			1.0E-05	1.0E-05	1.0E-04	4.0E-05

<b>Variant</b>	<b>Phenotype</b>	<b>Disease Relevance</b>	<b>Frequency</b>			<b>Average Frequency</b>
<b>G9E</b>	Unknown		1.0E-05	1.0E-05	1.0E-04	4.0E-05
<b>Leuven (E11K)</b>	Pathogenic (AD)	AD				
<b>V12I</b>	Unknown		1.0E-05	6.0E-05	2.0E-05	3.0E-05
<b>H13P</b>	Unknown					
<b>H14R</b>	Unknown		1.0E-05	1.0E-05		1.0E-05
<b>Q15E</b>	Unknown		1.0E-05			1.0E-05
<b>K16N</b>	Pathogenic (AD)	AD				
<b>V18M</b>	Unknown		1.0E-05	1.0E-05	2.0E-05	1.3E-05
<b>F19L</b>	Unknown					
<b>Flemish (A21G)</b>	Pathogenic (AD)	AD & CAA				
<b>E22D</b>	Unknown			1.0E-05		1.0E-05
<b>Osaka (E22Δ)</b>	Pathogenic (AD)	AD				
<b>Arctic (E22G)</b>	Pathogenic (AD)	AD & CAA				
<b>Dutch (E22Q)</b>	Pathogenic (CAA)	CAA				

<b>Variant</b>	<b>Phenotype</b>	<b>Disease Relevance</b>	<b>Frequency</b>			<b>Average Frequency</b>
<b>Italian (E22K)</b>	Pathogenic (AD)	CAA				
<b>Iowa (D23N)</b>	Pathogenic	AD & CAA				
<b>V24G</b>	Unknown		2.0E-05			2.0E-05
<b>V24A</b>	Unknown		2.0E-05			2.0E-05
<b>G25D</b>	Unknown					
<b>K28R</b>	Unknown		1.0E-05			1.0E-05
<b>I31V</b>	Unknown		2.0E-05	1.0E-05		1.5E-05
<b>I32V</b>	Unknown		1.0E-05	1.0E-05		1.0E-05
<b>Piedmont (L34V)</b>	Pathogenic (CAA)	CAA				
<b>V36M</b>	Unknown			1.0E-05		1.0E-05
<b>G38C</b>	Unknown			8.2E-06		8.2E-06
<b>G38S</b>	Not Pathogenic (AD)	PDD		4.1E-05		4.1E-05
<b>G38V</b>	Unknown			1.0E-05		1.0E-05
<b>V39I</b>	Unknown		2.0E-05	3.3E-05	1.0E-04	5.1E-05

Variant	Phenotype	Disease Relevance	Frequency			Average Frequency
I41V	Unknown					
A42T	Unknown	AD	1.0E-04	3.0E-05	5.8E-05	6.3E-05
A42V	Not Pathogenic (AD)		4.0E-05	2.0E-05	6.6E-06	4.2E-05



From the database search, a total of 20 A $\beta$  variants were found to meet the inclusion criteria. This included 13 pathogenic variants and 7 variants of not pathogenic or unknown significance. The developed comprehensive MRM method for variants within the A $\beta$ 42 sequence that met the inclusion criteria was listed in Table 7.

Table 7. MRM transitions of wt-A $\beta$ 40, wt-A $\beta$ 42, the ISs and the A $\beta$ 40 variants meeting the selection criteria for MRM development.

<b>Variant</b>	<b>Precursor ion (m/z)</b>	<b>Product ions (m/z)</b>
wt-A $\beta$ 40, E22K/D7N/E22Q/D23N/E11K*	1083	1054.1, 1029.1, 1000.8
wt-A $\beta$ 42	1129.4	1107.1, 1078.6, 1053.8
<sup>15</sup> N-IS-A $\beta$ 40	1096	1066.9
<sup>15</sup> N-IS-A $\beta$ 42	1143	1092.1
H6R	1088.2	1058.9, 1033.9, 1005.4
L34V/A21G/ K16N	1079.96	1050.5, 1011.5, 997.4
E22G	1065.45	1036.2, 1011.5, 997.1
E22 $\Delta$	1051.19	943.9, 914.8, 882.7
A2V	1090.4	1054.1, 1029.1, 1000.8
D7H	1089	1054.1, 1029.1, 948
G9A	1087	1050.5, 1029.1, 943.9
G9V	1093.3061	1054.1, 1029.1, 943.5
G9E	1101.5	1054.1, 1029.1, 1025.8

Variant	Precursor ion (m/z)	Product ions (m/z)
G38S	1090.9	1054.1, 1029.1, 1000.8
V39I	1087	1029.1, 1025.8, 1000.8
A42T	1137	1107.1, 1078.6, 1053.8
A42V	1136.5	1107.1, 1078.6, 1053.8

\* Variants separated chromatographically from wt- A $\beta$ 40

### 3.3.2 Heterozygous A $\beta$ Samples

By LC-MS/MS analysis, all nine A $\beta$  variants tested were resolved chromatographically from wt-A $\beta$ . For example, Figure 8 illustrates the heterozygote sample for the E22G variant. E22G resolved chromatographically from wt-A $\beta$ 40 and can be distinguished based on mass and by retention time. Additionally the E22G, D23N and E22Q variants co-eluted, with E22G readily identifiable by its unique MRMs. However, E22Q and D23N share precursor masses and transitions (as currently selected) within the prescribed m/z tolerances, and therefore if this MRM were present, would be reported as “E22Q or D23N variant” (Figure 10).

The example of variant E22Q is shown in Figure 9. E22Q has a similar molecular weight as wt-A $\beta$ 40, at 4,328.88 Da and 4,329.90 Da respectively. In a heterozygote sample containing E22Q and wt-A $\beta$ 40, the chromatogram of the E22Q variant MRM would demonstrate both the wt-A $\beta$ 40 and variant peaks. Fortunately, E22Q is resolved chromatographically from wt-A $\beta$ 40, that is, not located within each other’s respective MRM retention time windows. Thus, E22Q can be readily identified and distinguished from wt-A $\beta$ 40 in the LC-MS/MS assay.

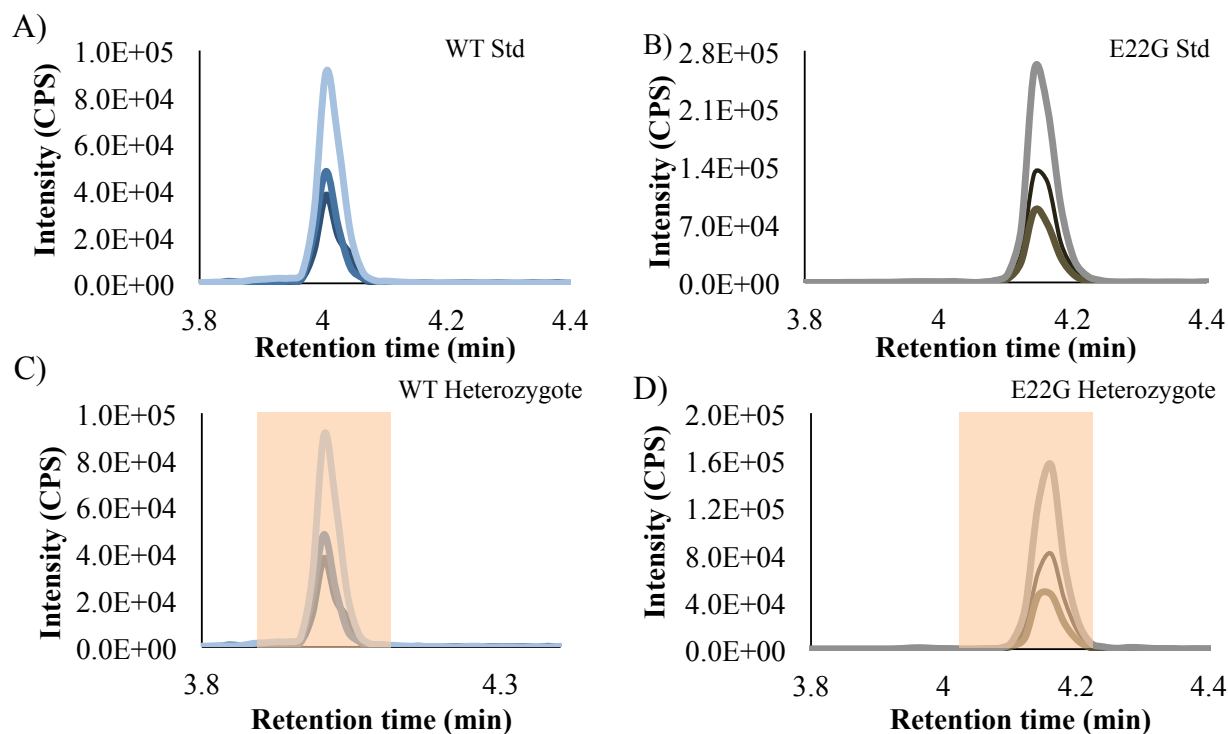


Figure 8: Wt-A $\beta$  peak and E22G variant can be distinguished based on mass and retention time.

Chromatograms of pure solutions of A) wt-A $\beta$ 40 and B) E22G variant. MRMs of the heterozygote CSF sample showing the (C) wt-A $\beta$ 40 MRM and the (D) E22G variant MRM, where the semi-transparent boxes indicate the retention time window considered for peak detection.

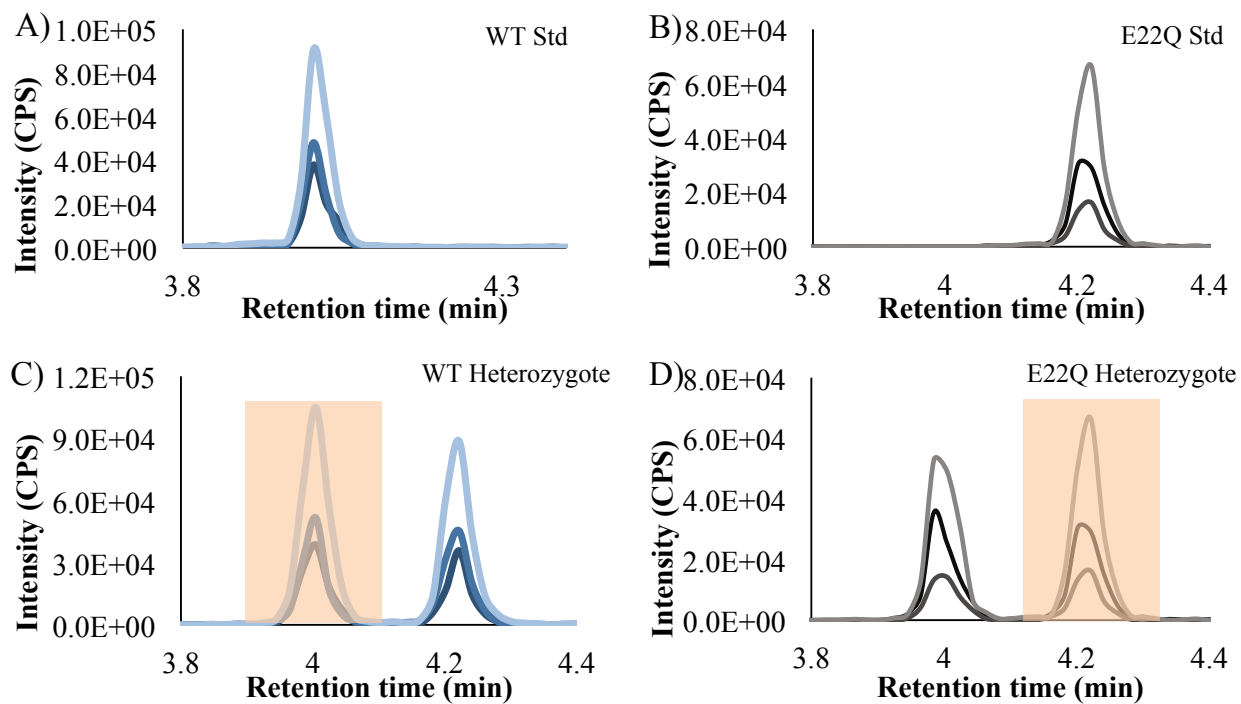


Figure 9: The variant E22Q was resolved chromatographically from wt-A $\beta$ . Chromatograms of pure solutions of A) wt-A $\beta$ 40 and B) E22Q variant. MRMs of the heterozygote CSF sample showing the (C) wt-A $\beta$ 40 MRM and (D) E22Q variant MRM, where the semi-transparent boxes indicate the retention time window considered for peak detection.

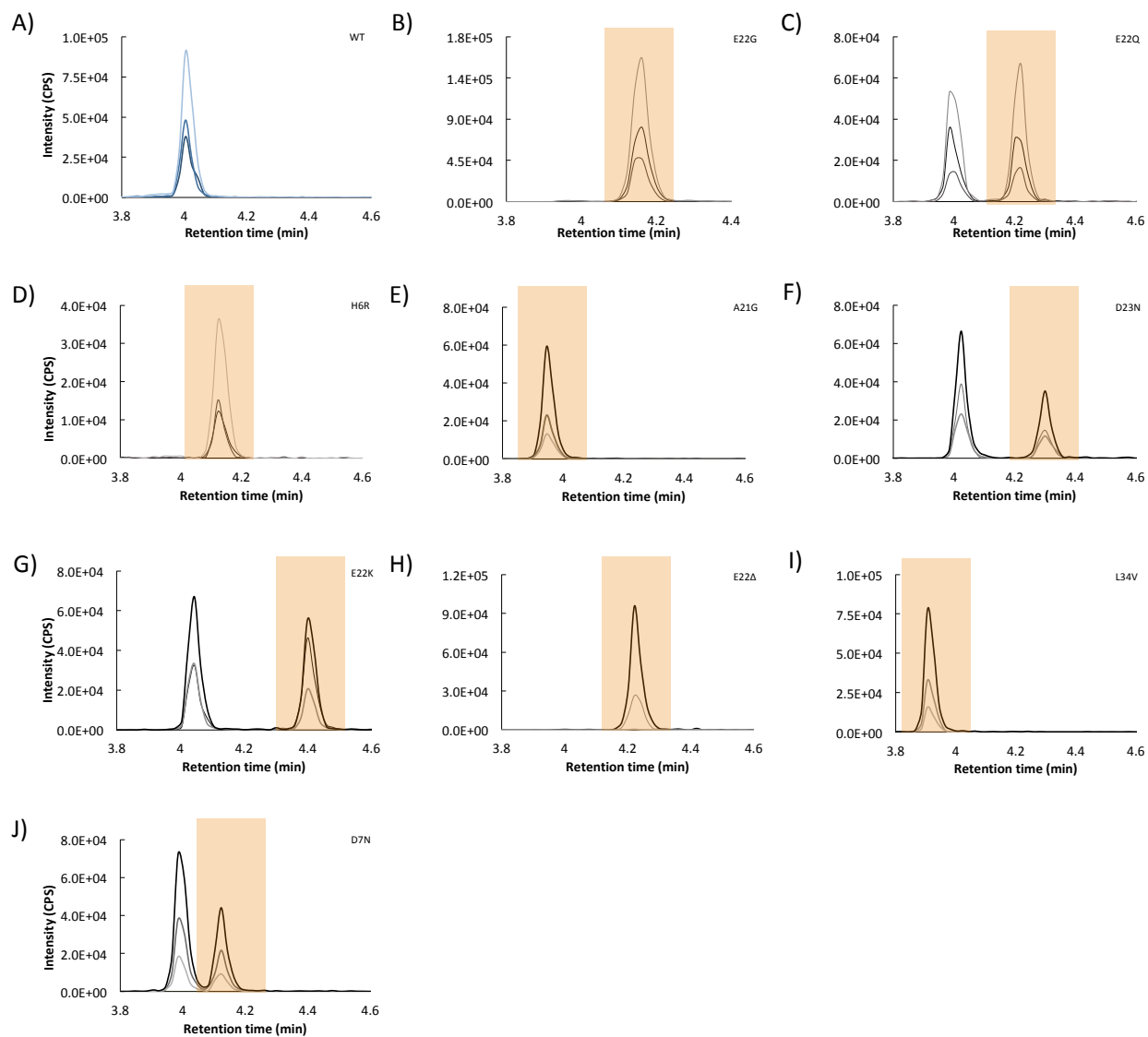


Figure 10: LC-MS/MS chromatograms of wt-Aβ40 (blue) and AD autosomal dominant variants (grey). A) Wt-Aβ40, B) Arctic (E22G), C) Dutch (E22Q), D) English (H6R), E) Flemish (A21G), F) Iowa (D23N), G) Italian (E22K), H) Osaka (E22Δ), I) Piedmont (L34V), J) Tottori (D7N). The semi-transparent boxes indicate the retention time window considered for peak detection.

### 3.4 Discussion

There are three types of variants: pathogenic, non-pathogenic, and unknown significance. Current MS methods for quantification of A $\beta$  have not been designed to identify these APP variants within the A $\beta$ 42 sequence [70-74, 84]. Due to LC-MS/MS being a highly selective analytical method, only peptides included in the MRM methods are observed. If present, such variants would be missed by the methods and total A $\beta$  content and quantification would be based on only the peptide arising from the wt allele. In the context of either a non-pathogenic variant or variant of unknown significance, a falsely low A $\beta$ 42 concentration would be reported, which could lead to a misdiagnosis of AD. Additionally screening for pathogenic variants can be used to identify autosomal dominant AD due to the variants being 100% penetrant. We thus adapted the multiplex A $\beta$  LC-MS/MS assay to identify all known variants occurring within the A $\beta$ 42 sequence. As proof of concept, CSF samples mimicking *APP* heterozygotes (one wt and one variant allele) were tested, demonstrated that the presence of variant A $\beta$  peptides could be readily identified. From this study, it was determined that using this adapted method, wt-A $\beta$  and variant A $\beta$  peptides can be distinguished by m/z ratios and/or retention time. For the remaining variants in the A $\beta$ 42 sequence that met our inclusion criteria, MRM parameters were developed for the LC-MS/MS assay.

### 3.5 Conclusion

The multiplex LC-MS/MS assay was adapted to quantify wt-A $\beta$ 42, A $\beta$ 40 and to identify A $\beta$  variants in CSF. Extension of this A $\beta$  multiplex LC-MS/MS assay to include known *APP* variants reflects an improvement in analytical accuracy, as the variants would be otherwise

missed and a falsely low A $\beta$  concentration reported. Additionally, including known pathogenic variants enables confirmatory diagnosis of autosomal dominant (i.e. familial) AD.

## Chapter 4: Summary

When developing assays in biological fluids, it is important to evaluate potential sources of analytical interference from both endogenous and exogenous sources. For the interference studies performed, the calculated % bias for the samples met the pre-specified criteria, indicating no interference for the endogenous and exogenous factors tested. Thus, the developed LC-MS/MS method was not susceptible to matrix interference from total protein content, hemolysate contamination, and immunoglobulins.

A limitation of existing LC-MS/MS methods for quantification of A $\beta$  is that they were designed to only identify wt peptides, which can lead to quantification errors in the presence of A $\beta$  variants and a missed opportunity to identify cases of autosomal dominant AD. Thus, the multiplex A $\beta$  LC-MS/MS assay was adapted to create an analytical tool suitable for accurate quantification of wt-A $\beta$ 40 and A $\beta$ 42 in CSF, as well as to identify presences of any of the known A $\beta$  variants occurring within the A $\beta$ 42 sequence. With this adaptation, the method can be used not only in its traditional role as to quantify biomarkers of AD pathology but also to identify cases of autosomal dominant AD. In addition, this method could be applied to further our understanding of A $\beta$  metabolism – differentiating wt and variant peptides – in autosomal dominant AD.



## References

- [1] International AsD. Dementia statistics.
- [2] Blennow K, de Leon MJ, Zetterberg H. Alzheimer's disease. *Lancet*. 2006;368:387-403.
- [3] Braak H, Braak E. Evolution of the neuropathology of Alzheimer's disease. *Acta Neurologia Scandinavica*. Supplement 165:3-12.
- [4] Serrano-Pozo A, Frosch MP, Masliah E, Hyman BT. Neuropathological Alterations in Alzheimer Disease. *Cold Spring Harbor Perspect Med*. 2011.
- [5] Glenner GG, Wong CW. Alzheimer's disease: initial report of the purification and characterization of a novel cerebrovascular amyloid protein. *Biochemical and biophysical research communications*. 1984;120:885-90.
- [6] Grundke-Iqbal I, Iqbal K, Quinlan M, Tung YC, Zaidi MS, Wisniewski HM. Microtubule-associated protein tau. A component of Alzheimer paired helical filaments. *The Journal of biological chemistry*. 1986;261:6084-9.
- [7] Kosik KS, Joachim CL, Selkoe DJ. Microtubule-associated protein tau (tau) is a major antigenic component of paired helical filaments in Alzheimer disease. *Proceedings of the National Academy of Sciences of the United States of America*. 1986;83:4044-8.
- [8] Haass C. Take five--BACE and the gamma-secretase quartet conduct Alzheimer's amyloid beta-peptide generation. *EMBO J*. 2004;23:483-8.
- [9] Portelius E, Price E, Brinkmalm G, Stiteler M, Olsson M, Persson R, et al. A novel pathway for amyloid precursor protein processing. *Neurobiology of aging*. 2011;32:1090-8.
- [10] Vassar R, Bennett BD, Babu-Khan S, Kahn S, Mendiaz EA, Denis P, et al. Beta-secretase cleavage of Alzheimer's amyloid precursor protein by the transmembrane aspartic protease BACE. *Science*. 1999;286:735-41.
- [11] Deshpande A, Mina E, Glabe C, Busciglio J. Different conformations of amyloid beta induce neurotoxicity by distinct mechanisms in human cortical neurons. *The Journal of neuroscience : the official journal of the Society for Neuroscience*. 2006;26:6011-8.
- [12] McLean CA, Cherny RA, Fraser FW, Fuller SJ, Smith MJ, Beyreuther K, et al. Soluble pool of Abeta amyloid as a determinant of severity of neurodegeneration in Alzheimer's disease. *Ann Neurol*. 1999;46:860-6.
- [13] Walsh DM, Selkoe DJ. A beta oligomers - a decade of discovery. *Journal of neurochemistry*. 2007;101:1172-84.

- [14] Haass C, Schlossmacher MG, Hung AY, Vigo-Pelfrey C, Mellon A, Ostaszewski BL, et al. Amyloid beta-peptide is produced by cultured cells during normal metabolism. *Nature*. 1992;359:322-5.
- [15] Olsson B, Lautner R, Andreasson U, Ohrfelt A, Portelius E, Bjerke M, et al. CSF and blood biomarkers for the diagnosis of Alzheimer's disease: a systematic review and meta-analysis. *The Lancet Neurology*. 2016;15:673-84.
- [16] Wolfe MS. Inhibition and modulation of gamma-secretase for Alzheimer's disease. *Neurotherapeutics : the journal of the American Society for Experimental NeuroTherapeutics*. 2008;5:391-8.
- [17] Gang Yu MN, Shigeki Arawaka, Diane Levitan, Lili Zhang, Anurag Tandon, You-Qiang Song, Ekaterina Rogaeva,, Fusheng Chen TK, Agnes Supala, Lyne Levesque, Haung Yu, Dun-Sheng Yang, Erin Holmes, Paul Milman,, Yan Liang DMZ, Dong Hong Xu, Christine Sato, Evgeny Rogaev, Marsha Smith, Christopher Janus, Yanni Zhang,, Ruedi Aebersold LF, Sandro Sorbi, Amalia Bruni, Paul Fraser & Peter St George-Hyslop. Nicastrin modulates presenilin-mediated notch/glp-1 signal transduction and  $\beta$ APP processing. *Nature*. 2000;407:48-54.
- [18] Wolfe MS, Xia W, Ostaszewski BL, Diehl TS, Kimberly WT, Selkoe DJ. Two transmembrane aspartates in presenilin-1 required for presenilin endoproteolysis and gamma-secretase activity. *Nature*. 1999;398:513-7.
- [19] Yu G, Nishimura M, Arawaka S, Levitan D, Zhang L, Tandon A, et al. Nicastrin modulates presenilin-mediated notch/glp-1 signal transduction and betaAPP processing. *Nature*. 2000;407:48-54.
- [20] Seubert P, Vigo-Pelfrey C, Esch F, Lee M, Dovey H, Davis D, et al. Isolation and quantification of soluble Alzheimer's beta-peptide from biological fluids. *Nature*. 1992;359:325-7.
- [21] Beher D, Wrigley JD, Owens AP, Shearman MS. Generation of C-terminally truncated amyloid-beta peptides is dependent on gamma-secretase activity. *Journal of neurochemistry*. 2002;82:563-75.
- [22] Xu F, Davis J, Miao J, Previti ML, Romanov G, Ziegler K, et al. Protease nexin-2/amyloid beta-protein precursor limits cerebral thrombosis. *Proceedings of the National Academy of Sciences of the United States of America*. 2005;102:18135-40.
- [23] Caille I, Allinquant B, Dupont E, Bouillot C, Langer A, Muller U, et al. Soluble form of amyloid precursor protein regulates proliferation of progenitors in the adult subventricular zone. *Development*. 2004;131:2173-81.
- [24] Conti L, Cattaneo E. Controlling neural stem cell division within the adult subventricular zone: an APpealing job. *Trends in neurosciences*. 2005;28:57-9.

- [25] Cordy JM, Hooper NM, Turner AJ. The involvement of lipid rafts in Alzheimer's disease. *Molecular membrane biology*. 2006;23:111-22.
- [26] Kerr ML, Small DH. Cytoplasmic domain of the beta-amyloid protein precursor of Alzheimer's disease: function, regulation of proteolysis, and implications for drug development. *Journal of neuroscience research*. 2005;80:151-9.
- [27] Hardy J, Selkoe DJ. The amyloid hypothesis of Alzheimer's disease: progress and problems on the road to therapeutics. *Science*. 2002;297:353-6.
- [28] Hardy JA, Higgins GA. Alzheimer's disease: the amyloid cascade hypothesis. *Science*. 1992;256:184-5.
- [29] Selkoe D. The molecular pathology of Alzheimer's disease. *Neuron*. 1991;6:487-98.
- [30] Selkoe DJ, Hardy J. The amyloid hypothesis of Alzheimer's disease at 25 years. *EMBO molecular medicine*. 2016;8:595-608.
- [31] Makin S. The amyloid hypothesis on trial. *Nature*. 2018;559:S4-S7.
- [32] Bertram L, Tanzi RE. The genetic epidemiology of neurodegenerative disease. *The Journal of clinical investigation*. 2005;115:1449-57.
- [33] Wolfe MS. When loss is gain: reduced presenilin proteolytic function leads to increased A $\beta$ 42/A $\beta$ 40. *EMBO reports*. 2007;8:136-40.
- [34] Tanzi RE, Bertram L. Twenty years of the Alzheimer's disease amyloid hypothesis: a genetic perspective. *Cell*. 2005;120:545-55.
- [35] Shepherd C, McCann H, Halliday GM. Variations in the neuropathology of familial Alzheimer's disease. *Acta neuropathologica*. 2009;118:37-52.
- [36] Levy-Lahad E, Wasco W, Poorkaj P, Romano DM, Oshima J, Pettingell WH, et al. Candidate gene for the chromosome 1 familial Alzheimer's disease locus. *Science*. 1995;269:973-7.
- [37] Rogaev EI, Sherrington R, Rogaeva EA, Levesque G, Ikeda M, Liang Y, et al. Familial Alzheimer's disease in kindreds with missense mutations in a gene on chromosome 1 related to the Alzheimer's disease type 3 gene. *Nature*. 1995;376:775-8.
- [38] Sherrington R, Rogaev EI, Liang Y, Rogaeva EA, Levesque G, Ikeda M, et al. Cloning of a gene bearing missense mutations in early-onset familial Alzheimer's disease. *Nature*. 1995;375:754-60.
- [39] Herreman A, Hartmann D, Annaert W, Saftig P, Craessaerts K, Serneels L, et al. Presenilin 2 deficiency causes a mild pulmonary phenotype and no changes in amyloid precursor protein

processing but enhances the embryonic lethal phenotype of presenilin 1 deficiency. *Proceedings of the National Academy of Sciences of the United States of America*. 1999;96:11872-7.

[40] Citron M, Oltersdorf T, Haass C, McConlogue L, Hung AY, Seubert P, et al. Mutation of the beta-amyloid precursor protein in familial Alzheimer's disease increases beta-protein production. *Nature*. 1992;360:672-4.

[41] Scheuner D, Eckman C, Jensen M, Song X, Citron M, Suzuki N, et al. Secreted amyloid beta-protein similar to that in the senile plaques of Alzheimer's disease is increased in vivo by the presenilin 1 and 2 and APP mutations linked to familial Alzheimer's disease. *Nature medicine*. 1996;2:864-70.

[42] Stenh C, Nilsberth C, Hammarback J, Engvall B, Naslund J, Lannfelt L. The Arctic mutation interferes with processing of the amyloid precursor protein. *Neuroreport*. 2002;13:1857-60.

[43] Jack CR, Jr., Bennett DA, Blennow K, Carrillo MC, Dunn B, Haeberlein SB, et al. NIA-AA Research Framework: Toward a biological definition of Alzheimer's disease. *Alzheimers Dement*. 2018;14:535-62.

[44] Mirra SS. The CERAD neuropathology protocol and consensus recommendations for the postmortem diagnosis of Alzheimer's disease: a commentary. *Neurobiology of aging*. 1997;18:S91-4.

[45] Braak H, Braak E. Neuropathological staging of Alzheimer-related changes. *Acta neuropathologica*. 1991;82:239-59.

[46] Knopman DS, DeKosky ST, Cummings JL, Chui H, Corey-Bloom J, Relkin N, et al. Practice parameter: diagnosis of dementia (an evidence-based review). Report of the Quality Standards Subcommittee of the American Academy of Neurology. *Neurology*. 2001;56:1143-53.

[47] Association AP. Diagnostic and statistical manual of mental disorders : DSM-5: American Psychiatric Association; 2013.

[48] McKhann G, Drachman D, Folstein M, Katzman R, Price D, Stadlan EM. Clinical diagnosis of Alzheimer's disease: report of the NINCDS-ADRDA Work Group under the auspices of Department of Health and Human Services Task Force on Alzheimer's Disease. *Neurology*. 1984;34:939-44.

[49] Husain MM, Garrett RK. Clinical diagnosis and management of Alzheimer's disease. *Neuroimaging clinics of North America*. 2005;15:767-77, ix-x.

[50] Consensus recommendations for the postmortem diagnosis of Alzheimer's disease. The National Institute on Aging, and Reagan Institute Working Group on Diagnostic Criteria for the Neuropathological Assessment of Alzheimer's Disease. *Neurobiology of aging*. 1997;18:S1-2.

- [51] Dubois B, Feldman HH, Jacova C, Hampel H, Molinuevo JL, Blennow K, et al. Advancing research diagnostic criteria for Alzheimer's disease: the IWG-2 criteria. *The Lancet Neurology*. 2014;13:614-29.
- [52] Blennow K, Mattsson N, Scholl M, Hansson O, Zetterberg H. Amyloid biomarkers in Alzheimer's disease. *Trends in pharmacological sciences*. 2015;36:297-309.
- [53] Klunk WE, Engler H, Nordberg A, Wang Y, Blomqvist G, Holt DP, et al. Imaging brain amyloid in Alzheimer's disease with Pittsburgh Compound-B. *Ann Neurol*. 2004;55:306-19.
- [54] Allen M, Zou F, Chai HS, Younkin CS, Crook J, Pankratz VS, et al. Novel late-onset Alzheimer disease loci variants associate with brain gene expression. *Neurology*. 2012;79:221-8.
- [55] Tolboom N, van der Flier WM, Yaqub M, Boellaard R, Verwey NA, Blankenstein MA, et al. Relationship of Cerebrospinal Fluid Markers to 11C-PiB and 18F-FDDNP Binding. *The Journal of Nuclear Medicine*. 2009;50:1464-70.
- [56] Forsberg A, Engler H, Almkvist O, Blomqvist G, Hagmanb G, Wall A, et al. PET imaging of amyloid deposition in patients with mild cognitive impairment. *Neurobiology of aging*. 2008;29:1456-65.
- [57] Ye L, Morgenstern JL, Gee AD, Hong G, Brown J, Lockhart A. Delineation of positron emission tomography imaging agent binding sites on beta-amyloid peptide fibrils. *The Journal of biological chemistry*. 2005;280:23599-604.
- [58] Maruyama M, Shimada H, Suhara T, Shinotoh H, Ji B, Maeda J, et al. Imaging of tau pathology in a tauopathy mouse model and in Alzheimer patients compared to normal controls. *Neuron*. 2013;79:1094-108.
- [59] Chien DT, Szardenings AK, Bahri S, Walsh JC, Mu F, Xia C, et al. Early clinical PET imaging results with the novel PHF-tau radioligand [F18]-T808. *Journal of Alzheimer's disease : JAD*. 2014;38:171-84.
- [60] Rowe CC, Ackerman U, Browne W, Mulligan R, Pike KL, O'Keefe G, et al. Imaging of amyloid beta in Alzheimer's disease with 18F-BAY94-9172, a novel PET tracer: proof of mechanism. *The Lancet Neurology*. 2008;7:129-35.
- [61] Mo J. Cerebrospinal Fluid f'-Amyloid1-42 Levels in the Differential Diagnosis of Alzheimer's Disease - Systematic Review and Meta-Analysis. *Value in health : the journal of the International Society for Pharmacoeconomics and Outcomes Research*. 2014;17:A391.
- [62] Fagan AM, Mintun MA, Mach RH, Lee S, Dence CS, Shah AR, et al. Inverse Relation between In Vivo Amyloid Imaging Load and Cerebrospinal Fluid AB42 in Humans. *Ann Neurol*. 2006;59:512-9.

- [63] Grimmer T, Riemenschneider M, Förstl H, Henriksen G, Klunk WE, Mathis CA, et al. Beta Amyloid in Alzheimer's Disease: Increased Deposition in Brain Is Reflected in Reduced Concentration in Cerebrospinal Fluid. *Biological psychiatry*. 2009;65:927-34.
- [64] Scahill RI, Schott JM, Stevens JM, Rossor MN, Fox NC. Mapping the evolution of regional atrophy in Alzheimer's disease: Unbiased analysis of fluid-registered serial MRI. *PNAS*. 2002;99:4703-7.
- [65] Killiany RJ, Hyman BT, Gomez-Isla T, Moss MB, Kikinis R, Jolesz F, et al. MRI measures of entorhinal cortex vs hippocampus in preclinical AD. *Neurology*. 2002;58:1188-96.
- [66] Lehericy S, Baulac M, Chiras J, Pierot L, Martin N, Pillon B, et al. Amygdalohippocampal MR volume measurements in the early stages of Alzheimer disease. *AJNR American journal of neuroradiology*. 1994;15:929-37.
- [67] Chan D, Fox NC, Scahill RI, Crum WR, Whitwell JL, Leschziner G, et al. Patterns of temporal lobe atrophy in semantic dementia and Alzheimer's disease. *Ann Neurol*. 2001;49:433-42.
- [68] Logothetis NK, Pauls J, Augath M, Trinath T, Oeltermann A. Neurophysiological investigation of the basis of the fMRI signal. *Nature*. 2001;412:150-7.
- [69] Gusnard DA, Raichle ME, Raichle ME. Searching for a baseline: functional imaging and the resting human brain. *Nature reviews Neuroscience*. 2001;2:685-94.
- [70] Magdalena Korecka TW, Michal Figurski, Jon B. Toledo, Steven E. Arnold, Murray Grossman, John Q. Trojanowski, and Leslie M. Shaw. Qualification of a Surrogate Matrix-Based Absolute Quantification Method for Amyloid- $\beta$ 42 in Human Cerebrospinal Fluid Using 2D UPLC-Tandem Mass Spectrometry. *Journal of Alzheimer's disease*. 2014;41:441-51.
- [71] Mattsson N, Andreasson U, Persson S, Carrillo MC, Collins S, Chalbot S, et al. CSF biomarker variability in the Alzheimer's Association quality control program. *Alzheimer's & Dementia*. 2013;9:251-61.
- [72] Ping-ping Lin W-IC, Fei Yuan, Lei Sheng, Yu-jia Wu, Wei-wei Zhang, Guo-qing Li, Hong-rong Xu, Xue-ning Li. An UHPLC-MS/MS method for simultaneous quantification of human amyloid beta peptides A $\beta$ 1-38, A $\beta$ 1-40 and A $\beta$ 1-42 in cerebrospinal fluid using micro-elution solid phase extraction. *Journal of Chromatography B*. 2017;1070:82-91.
- [73] Shaw LM, Vanderstichele H, Knapik-Czajka M, Figurski M, Coart E, Blennow K, Soares H, Simon A.J., Lewczuk P, Dean R.A., Siemers E, Potter W, Lee V.M.Y., Trojanowski J.Q., and Alzheimer's Disease Neuroimaging Initiative. Qualification of the analytical and clinical performance of CSF biomarker analyses in ADNI. *Acta Neuropathol* 2011;121:597-609.

- [74] Mary E. Lame EEC, Matthew Blatnik Quantitation of amyloid beta peptides Ab1–38, Ab1–40, and Ab1–42 in human cerebrospinal fluid by ultra-performance liquid chromatography–tandem mass spectrometry. *Analytical biochemistry*. 2011;419:133-9.
- [75] Dimeski G. Interference testing. *The Clinical biochemist Reviews*. 2008;29 Suppl 1:S43-8.
- [76] Nikolac N. Lipemia: causes, interference mechanisms, detection and management. *Biochemia medica*. 2014;24:57-67.
- [77] Bogstedt A, Groves M, Tan K, Narwal R, McFarlane M, Hoglund K. Development of Immunoassays for the Quantitative Assessment of Amyloid-beta in the Presence of Therapeutic Antibody: Application to Pre-Clinical Studies. *Journal of Alzheimer's disease : JAD*. 2015;46:1091-101.
- [78] Vanderstichele H, Stoops E, Vanmechelen E, Jeromin A. Potential sources of interference on Abeta immunoassays in biological samples. *Alzheimers Res Ther*. 2012;4:39.
- [79] Ellis MJ, Livesey JH. Techniques for identifying heterophile antibody interference are assay specific: study of seven analytes on two automated immunoassay analyzers. *Clin Chem*. 2005;51:639-41.
- [80] Emerson JF, Ngo G, Emerson SS. Screening for interference in immunoassays. *Clin Chem*. 2003;49:1163-9.
- [81] Grebe SK, Singh RJ. LC-MS/MS in the Clinical Laboratory - Where to From Here? *The Clinical biochemist Reviews*. 2011;32:5-31.
- [82] Skoog DA, Holler JF, Crouch SR. *Principles of Instrumental Analysis* 6th ed. United States of America: Brooks/Cole; 2007.
- [83] Khoonsari PE, Häggmark, A., Lönnberg, M., Mikus, M., Kilander, L., Lannfelt, L., Bergquist, J., Ingelsson, M., Nilsson, P., Kulima, K., Shevchenko, G. Analysis of the Cerebrospinal Fluid Proteome in Alzheimer's Disease. *PloS one*. 2016;11.
- [84] Leinenbach A, Pannee J, Dulffer T, Huber A, Bittner T, Andreasson U, et al. Mass spectrometry-based candidate reference measurement procedure for quantification of amyloid-beta in cerebrospinal fluid. *Clin Chem*. 2014;60:987-94.
- [85] Blennow K, Hampel H, Zetterberg H. Biomarkers in amyloid-beta immunotherapy trials in Alzheimer's disease. *Neuropsychopharmacology : official publication of the American College of Neuropsychopharmacology*. 2014;39:189-201.
- [86] van Dyck CH. Anti-Amyloid-b Monoclonal Antibodies for Alzheimer's Disease: Pitfalls and Promise. *Biological psychiatry*. 2018;83:311-9.
- [87] Blennow K. Biomarkers in Alzheimer's disease drug development. *Nature medicine*. 2010;16:1218-22.

- [88] Jack CR, Jr., Knopman DS, Jagust WJ, Shaw LM, Aisen PS, Weiner MW, et al. Hypothetical model of dynamic biomarkers of the Alzheimer's pathological cascade. *The Lancet Neurology*. 2010;9:119-28.
- [89] van der Gugten GJ, Fok AC, Hsiung GR, DeMarco ML. Automated mass spectrometric method for identification and quantitation of wild-type and familial variants of amyloid-beta peptides in cerebrospinal fluid. *Journal of the Alzheimer's Association* 2016;12:477-8.
- [90] CLSI. Evaluation of the Linearity of Quantitative Measurement Procedures: A Statistical Approach; Approved Guideline. CLSI document EP6-A. Wayne, PA: Clinical and Laboratory Standards Institute 2003.
- [91] CLSI. Evaluation of Precision of Quantitative Measurement Procedures; Approved Guideline. CLSI document EP-5A. 3 ed. Wayne, PA: Clinical and Laboratory Standards Institute; 2014.
- [92] CLSI. Liquid Chromatography-Mass Spectrometry Methods; Approved Guideline. CLSI document C62-A. Wayne, PA: Clinical and Laboratory Standards Institute; 2014.
- [93] Vanderstichele H, Stoops, E., Vanmechelen, E. and Jeromin, A. Potential sources of interference on Abeta immunoassays in biological samples. *Alzheimer's Research & Therapy*. 2012;4.
- [94] Jeffrey L. Cummings S, Sharon Cohen, Christopher H. van Dyck, Mark Brody, Craig Curtis WC, Michael Ward, Michel Friesenhahn, Christina Rabe, , Flavia Brunstein AQ, Lee A. Honigberg, Reina N. Fuji, David Clayton DM, Carole Ho, and Robert Paul. A phase 2 randomized trial of crenezumab in mild to moderate Alzheimer disease. *Neurology*. 2018;90:e1889-e97.
- [95] Hooshfar S, Basiri B, Bartlett MG. Development of a surrogate matrix for cerebral spinal fluid for liquid chromatography/mass spectrometry based analytical methods. *Rapid communications in mass spectrometry : RCM*. 2016;30:854-8.
- [96] McCudden CR, Brooks J, Figurado P, Bourque PR. Cerebrospinal Fluid Total Protein Reference Intervals Derived from 20 Years of Patient Data. *Clin Chem*. 2017;63:1856-65.
- [97] MacLean B, Tomazela DM, Shulman N, Chambers M, Finney GL, Frewen B, et al. Skyline: an open source document editor for creating and analyzing targeted proteomics experiments. *Bioinformatics*. 2010;26:966-8.